

THESIS

ANTIBACTERIAL EFFECTS OF SPUTTER DEPOSITED SILVER-DOPED  
HYDROXYAPATITE THIN FILMS

Submitted by

Nathan Anthony Trujillo

Graduate Degree Program in Bioengineering

In partial fulfillment of the requirements

For the Degree of Master of Science

Colorado State University

Fort Collins, Colorado

Spring 2011

Master's Committee:

Advisor: Ketul Popat

Co-Advisor: John Williams

Debbie Crans

Melissa Reynolds

## ABSTRACT

### ANTIBACTERIAL EFFECTS OF SPUTTER DEPOSITED SILVER-DOPED HYDROXYAPATITE THIN FILMS

Over recent years, researchers have studied innovative ways to increase the lifespan of orthopedic implants in order to meet the soaring demand of hip and knee replacements. Since many of these implants fail as a result of loosening, wear, and inflammation caused by repeated loading on the joints, coatings such as hydroxyapatite (HAp) on titanium with a unique topography have been shown to improve the interface between the implant and the natural tissue. Other serious problems with long-term or ideally permanent implants are bacterial colonization. It is important to prevent initial bacterial colonization as existing colonies have potential to become encased in an extracellular matrix polymer (biofilm) which is resistant to antibacterial agents. The following work considers the potential of etching using plasma based ion implantation and ion beam sputter deposition to produce hydroxyapatite thin films on etched titanium doped with silver as an antibacterial component.

Plasma-based ion implantation was used to examine the effects of pre-etching on plain titanium. Topographical changes to the titanium samples were examined and compared via scanning electron microscopy. It was determined that plasma-based ion implantation at  $-700\text{eV}$  could etch titanium to produce similar topography as ion beam etching in a shorter processing time. Hydroxyapatite and silver-doped hydroxyapatite thin

films were then sputter deposited on titanium substrates etched at -700eV. For silver-doped films, two concentrations of silver (~0.5wt% and ~1.5wt%) were used. Silver concentrations in the film were determined using energy dispersive x-ray spectroscopy. Film thicknesses were determined by measuring the surface profile using contact profilometry.

*Staphylococcus epidermidis* (SE) and *Pseudomonas aeruginosa* (PA) adhesion studies were performed on plain titanium, titanium coated with hydroxyapatite, titanium coated with ~0.5 wt% silver-doped hydroxyapatite, and titanium coated with ~1.5wt% silver-doped hydroxyapatite. It was discovered during the study that the films were delaminating from the samples thus killing bacteria in suspension. Release studies performed in addition to adhesion confirmed that the silver-doped films prevented SE and PA bacterial growth in suspension. To prevent delamination, the films were annealed by heat treatment in air at a temperature of 600°C. X-ray diffraction confirmed the presence of a crystalline hydroxyapatite phase on each sample type. Films were immersed in PBS at 37°C and remained in incubation for four weeks to determine there was no delamination or silver leaching.

## ACKNOWLEDGEMENTS

There are many people without whom this thesis would not have been possible. First and foremost, I would like to thank my family. To my parents, Ron and Debbie, thank you so much for your love and for believing that I could achieve whatever goals I set for myself. To my sister and brother, Nicole and Noah, thank you for giving me encouragement when I've needed it most. Many thanks go out to my extended family as well for their love and support throughout this journey.

I especially wish to thank my advisors, Dr. Ketul Popat and Dr. John Williams for allowing me to work in their labs and for providing me with a wealth of knowledge as I've worked with them on this project. Their insight, leadership, and guidance have greatly increased my interest and understanding of biomaterials and plasma engineering. Thank you to Dr. Melissa Reynolds and Dr. Debbie Crans for serving as my committee members and for taking the time to review this thesis outside of their demanding schedules.

A great deal of thanks goes to Dr. Rachael Oldinski and her graduate student Hongyan Ma from University of Washington for collaborating with me to complete the bacterial studies on my samples. This thesis would not have been possible without their extraordinary help. Thank you to my colleagues in the CEPPE Lab, Dr. Casey Farnell, Dr. Cody Farnell, and Nick Riedel for their immense help and advice on vacuum technology, plasma etching, and ion beam sputtering. In addition, thank you to Plasma

Controls for allowing me to work on this project in conjunction with both labs at CSU. Thank you to Daisy Williams for her ideas and assistance with lab maintenance, experimental set-up, and for helping this project to run as smoothly as possible.

Finally, thank you to my friends in the CEPPE Lab and the BSμηEL for showing me every day how important it is to have fun while working hard. I would especially like to thank all my many friends here in Fort Collins who up-lift me every day through their inspiration, fellowship, and support.

## TABLE OF CONTENTS

CHAPTER 1: INTRODUCTION AND BACKGROUND .....	1
CHAPTER 2: PLASMA AND ION BEAM PROCESSING METHODS.....	7
2.1: <i>SUBSTRATE AND TARGET PREPARATION</i> .....	7
2.2: <i>PLASMA REACTOR DESIGN AND DEVELOPMENT</i> .....	9
2.3: <i>PLASMA PRE-ETCH OF TITANIUM SUBSTRATES</i> .....	11
2.4: <i>ION BEAM SPUTTER DEPOSITION OF THIN FILMS</i> .....	13
CHAPTER 3: PHYSICAL AND MECHANICAL CHARACTERIZATION OF THE THIN FILMS .....	15
3.1: <i>METHODS AND MATERIALS</i> .....	15
3.2: <i>RESULTS AND DISCUSSION</i> .....	19
CHAPTER 4: BACTERIAL RESPONSE OF THE SILVER-DOPED HYDROXYAPATITE THIN FILMS.....	29
4.1: <i>METHODS AND MATERIALS</i> .....	29
4.2: <i>RESULTS AND DISCUSSION</i> .....	32
CHAPTER 5: PRELIMINARY ANNEALING AND HIGH TEMPERATURE TREATMENTS OF THE THIN FILMS .....	45
5.1: <i>METHODS AND MATERIALS</i> .....	45
5.2: <i>RESULTS AND DISCUSSION</i> .....	48
CHAPTER 6: CONCLUSIONS AND FUTURE WORK.....	56
WORKS CITED .....	58

## LIST OF FIGURES

Figure 1: Plasma-based ion implantation and surface bombardment .....	5
Figure 2: Ion beam sputter deposition .....	6
Figure 3: Sputtering target of sintered hydroxyapatite tiles.....	9
Figure 4: Plasma source assembly .....	11
Figure 5: Wiring schematic of the plasma source.....	13
Figure 6: Surface profile of film thickness using contact profilometry.....	19
Figure 7: -700eV Etched Titanium Substrates at 1000x, 5000x and 25000x .....	20
Figure 8: Micro-scale topography from plasma (left) and ion beam (right) processing...	21
Figure 9: Comparison between unmodified Ti and etched Ti coated with HAp + Ag.....	21
Figure 10: Weight percentages of silver in the hydroxyapatite films.....	23
Figure 11: Spectral imaging of substrate groups A1 and A2.....	24
Figure 12: ASTM D3359 Adhesion by Tape Test.....	25
Figure 13: Delaminated films after PBS immersion for 4 weeks .....	26
Figure 14: Film Delamination at 1000x and 10000x .....	27
Figure 15: Evaluation of silver wt% before and after stability studies.....	28
Figure 16: Bacteria adhesion of <i>SE</i> : Dead cells.....	32
Figure 17: Bacteria adhesion of <i>SE</i> : Live cells.....	33
Figure 18: Bacterial adhesion of <i>SE</i> : % of Dead cells .....	34
Figure 19: Bacterial adhesion of <i>PA</i> : Dead cells .....	35

Figure 20: Bacterial adhesion of <i>PA</i> : Live cells .....	35
Figure 21: Bacterial adhesion of <i>PA</i> : % of Dead cells.....	36
Figure 22: <i>SE</i> and <i>PA</i> cells on plain titanium .....	38
Figure 23: <i>SE</i> and <i>PA</i> on etched titanium coated with HAp.....	39
Figure 24: <i>SE</i> and <i>PA</i> on etched titanium coated with 0.5% silver-doped HAp .....	41
Figure 25: <i>SE</i> and <i>PA</i> on etched titanium coated with 1.5% silver-doped HAp .....	42
Figure 26: Growth of <i>SE</i> bacteria cells over 8 hours in solution .....	43
Figure 27: Growth of <i>PA</i> bacteria cells over 8 hours in solution.....	44
Figure 28: High temperature sample holder with installed heater cartridges .....	47
Figure 29: Substrates subjected to high temperature during sputter deposition .....	49
Figure 30: Comparison of amorphous and crystalline silver-doped HAp thin films.....	50
Figure 31: Spectral imaging of substrate groups A3 and A4.....	51
Figure 32: SEM images of annealed silver-doped hydroxyapatite films on etched Ti.....	52
Figure 33: XRD scan of annealed 0.5 wt% silver-doped hydroxyapatite film substrate..	53
Figure 34: XRD scan of annealed 1.5 wt% silver-doped hydroxyapatite film substrate..	54
Figure 35: No delamination or damage of the annealed film from PBS immersion .....	55
Figure 36: Comparison of silver wt% before and after 4 week stability studies in PBS..	55

## LIST OF TABLES

Table 1: Substrate group labels and descriptions.....	8
Table 2: Annealed substrate group labels and descriptions .....	48

## CHAPTER 1: INTRODUCTION AND BACKGROUND

In recent years, the number of implanted internal fixation devices and total joint arthroplasties has seen an increasing trend in the United States. Today more than 4.4 million people have an internal fixation device and over 1.3 million people possess an artificial joint [1]. Since orthopedic procedures have become so common, it is believed that nearly 600,000 total hip replacements and 1.4 million knee replacements surgeries will be completed in the year 2015 [2]. Not only is there high demand of orthopedic surgeries for new patients every year, there is an even higher demand for patients who must receive revision surgeries. Although most implants will last up to 20 years in more than 80% of the patient population, there is a subset of patients who will need to endure a revision surgery within 5 years after the procedure for both hip and knee replacements [3-5]. Common problems associated with patients who require revision surgeries are instability, aseptic loosening, infection, wear, osteolysis, ingrowth failure, and periprosthetic fracture [4, 5].

Titanium and its alloys are widely used in orthopedic devices due to their biocompatibility with bone tissue, resistance to corrosion, high strength, and high modulus of elasticity [6]. The long term success of orthopedic biomaterials is greatly dependent on effective osseointegration of the tissue with the implant as well as the existence of a sterile environment to reduce the risk of bacterial infections [7]. Osseointegration requires the cooperation of multiples cell and tissue types and is intended to mimic tissue fracture repair [8]. Although titanium and its alloys are near

ideal biomaterials, their use does not always guarantee adequate results. Orthopedic implants are currently unpredictable due to incomplete osseointegration which increases the risk of implant loosening. Efforts to improve host cell-implant interaction have been investigated to enhance osseointegration [6]. Unmodified titanium is prone to bacterial infections which may eventually lead to inflammation and destructive failure of the implant. It is well recognized that prevention of initial bacterial adhesion is critical to inhibit biofilm formation [9].

Calcium phosphate, and its counterparts such as hydroxyapatite (HAp) with a chemical formula of  $\text{Ca}_5(\text{PO}_4)_3\text{OH}$ , is a biocompatible and bioactive material which is known to make up nearly 60-70% of the inorganic portion of the bone matrix. In addition, it also constitutes to the mechanical strength of the tissue [10-13]. Hydroxyapatite was first used by Furlong and Osborn in 1985 during clinical trials which showed increased osseointegration after the new implants began interacting with the bone after only 10 day post insertions [14,15]. Since that time, hydroxyapatite has been widely studied and used in many in-vivo studies using animal models to examine the efficiency of hydroxyapatite coated devices for enhanced stability and interaction with the natural bone tissue [15]. The level of integration between the coated implants and the natural bone tissue is a result of the biomimetic properties of the hydroxyapatite coating in terms of chemical composition, surface properties, mechanical properties, and grain structure [13, 16]. In addition to animal models, documented medical reviews have reported that in both total hip and total knee arthroplasties in humans, the use of hydroxyapatite coating has been shown to increase the interaction and osseointegration of bio-inert metal implants [17-21].

In addition to loosening of the hardware, failure of orthopedic implants also result from bacterial infections from both Gram-positive and Gram-negative pathogens. *Staphylococcus Epidermis (SE)* and *Pseudomonas Aeruginosa (PA)* are Gram-positive and Gram-negative microbes, respectively. *SE* is known to be involved in approximately 30% of all bacterial colonies that form in orthopedic implants [22, 23]. Due to low sterility, skin is the most common source of the staphylococcus species which is responsible for 60% of all prosthetic infections, not just orthopedic [24]. *PA* is the most common Gram-negative non-*staphylococcus* bacterial strain found in orthopedic infections [23]. Although Gram-negative aerobe infections are not as common as infections from Gram-positive strains, they are still very dangerous if growth is allowed to continue and biofilms are allowed to form. *PA* prosthetic and bone infections are difficult and often require two-stage revision surgeries as the primary treatment [25]. Often times prophylactic antibiotic administration to the area where the implant was placed has been shown reduce the incidence and amount of infection if one was to occur [24, 26]. However the cost of doing so is significant even if the risk of infection is very low [27]. If infection does occur, today the most common therapy for prosthetic joint infection is two-stage implant exchange partnered with 6 weeks of intravenous antibiotic administration resulting in long periods of hospitalization [25].

Silver has been known to be used in many medical devices such as bone cements, catheters, orthopedic fixation pins, dental implants, and cardiac prostheses [28]. One of the best known uses for the use of silver in medicine has been to serve as the primary antimicrobial agent in the healing severe burns through treatments such as topical creams [29, 30]. The antimicrobial properties of silver have a high dependence on the release of

the silver ion  $\text{Ag}^+$  from metallic silver and other silver compounds such as silver sulfadiazine which help keep the silver in a stable form [28, 31]. Since bacterial infection is a major problem with prosthetic failures, over the years silver has been considered as a medical coating since it exhibits a broad range of antimicrobial activity and bacterial inactivation in-vitro. Such activities include binding to microbial DNA which prevents bacterial replication and binding to the sulfhydryl groups of the electron transport chain metabolic enzymes which in turn inactivates those enzymes [1, 32]. Since it is desired to obtain a coating that has antimicrobial properties and helps with osseointegration of the tissue with the implant, silver-doped hydroxyapatite coatings have been attempted using methods such as sol-gel, physical vapor deposition, and plasma spraying [33-35].

The alternative process method which is considered in this study is a combination of plasma-based ion implantation (etching) and ion beam sputter deposition. Previous work has shown that ion beam sputtering is an effective method for producing high quality hydroxyapatite thin films [15, 36-39]. Coupling ion beam sputtering with plasma-based etching, it is possible to produce a surface on the substrate that has a unique topography with a thin film coating with the necessary elements to help osseointegration and inhibit bacterial growth. Plasma-based etching or plasma based ion implantation is a method which begins by placing a substrate in a vacuum environment while the chamber is back-filled an inert gas such as argon. A plasma discharge is created by heating the gas atoms which causes them to be ionized. The resulting plasma contains charged particles of both positive gas ions and negative electrons. While the substrate is immersed in the plasma, the substrate is biased to a negative voltage which attracts the excited ions and causes them to accelerate towards the substrate at high velocities. Once the ions impact

the substrate, they disrupt the surface structure at an atomic level and their energy subsequently causes particles of the substrate to expel off the surface (Figure 1). These expelled (sputtered) particles travel away from the substrate until they make contact with a different surface in the vacuum chamber. This process of ion bombardment leaves behind a surface topography at micro and nano-scale levels that is very distinctive.

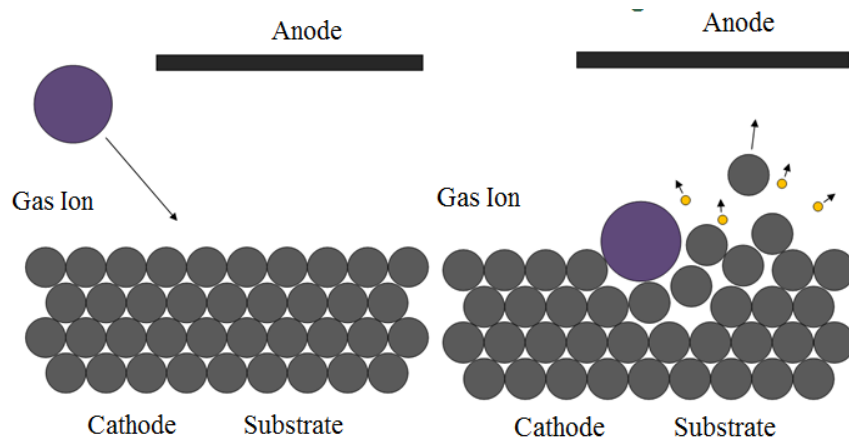


**Figure 1:** Plasma-based ion implantation and surface bombardment

Ion beam sputter deposition is a similar method to plasma-based ion implantation except that the target is bombarded by a beam of energetic ions which are produced from inside an ion source. The discharge chamber of the ion source is filled with a process gas where the gas atoms are ionized and a plasma discharge is formed inside containing charged particles. The ionized atoms are accelerated through set of grids which are biased at specific voltages in order to expel the ions from the source at a high velocity as shown in Figure 2. A neutralizer is placed downstream from the ion source in order to balance the ion beam with negative electrons. As with plasma-based ion implantation, the ions bombard the surface of the target which causes particles to be disturbed and eject from the surface causing them to be sputtered on other surfaces within the vacuum chamber. The direction at which the particles travel depends on the angle at which they were

impacted. As sputtered particles are collected on the near-by surfaces, ultimately a thin film is formed. The following work studies the possibility of using plasma-based etching and ion beam sputter deposition to create surface with a unique topography and coat those surfaces with silver-doped hydroxyapatite thin films to prevent bacterial growth and colonization.

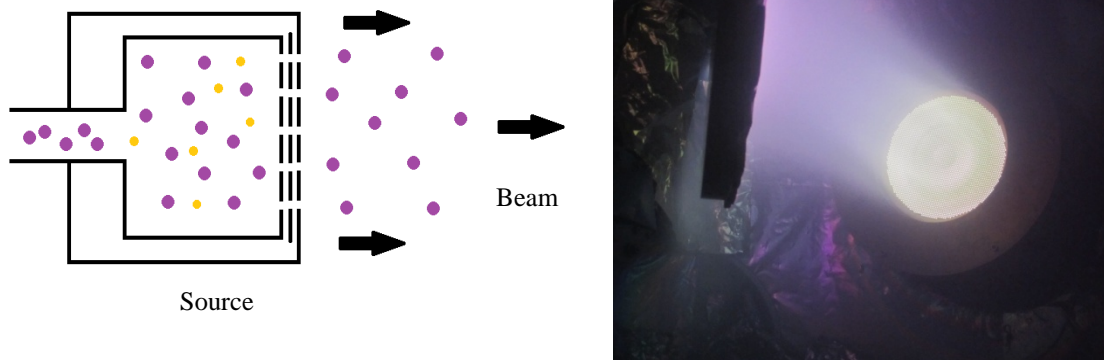


**Figure 2:** Ion beam sputter deposition

## CHAPTER 2: PLASMA AND ION BEAM PROCESSING METHODS

The following chapter discusses the methods used for preparing the titanium substrates for plasma processing and the hydroxyapatite sputtering target. In addition, this chapter will give an overview of the design and fabrication of the plasma reactor system along with the procedures used to etch the titanium substrates and sputter coat thin films using ion beam processing.

### 2.1: SUBSTRATE AND TARGET PREPARATION

Substrates for deposition were prepared from ASTM Grade 1 commercially pure (CP4) titanium sheets cut into 1cm by 1cm squares with a thickness of 0.060 in. Grade 1 titanium is very commonly used in medical applications in addition to the titanium-aluminum-vanadium alloy, Ti<sub>6</sub>Al<sub>4</sub>V ELI (extra low interstitial). The 1cm by 1cm titanium substrates were deburred, cleaned, and stored for future use. The cleaned substrates were separated into the four different test groups (Table 1) and marked using a scribe. The two control groups in this study were unmodified as-received titanium (T) and etched titanium sputter coated with hydroxyapatite only (H). The two primary test groups were etched titanium sputter coated with hydroxyapatite doped with a low concentration of silver (A1) and etched titanium sputter coated with hydroxyapatite doped with a high concentration of silver (A2). The titanium substrates were handled using nitrile gloves at all times and carefully stored to prevent unwanted surface contamination.

**Table 1:** Substrate group labels and descriptions

<b>Substrate Label</b>	<b>T</b>	<b>H</b>	<b>A1</b>	<b>A2</b>
<b>Description</b>	Unmodified As-received Ti	Etched Ti + Sputtered HAp	Etched Ti + Sputtered HAp + Low wt% Ag	Etched Ti + Sputtered HAp + High wt% Ag

Calcium phosphate tribasic (hydroxyapatite) powder (Alfa Aesar, CAS #12167-74-7) was placed into an aluminum die and pressed to create 1.5 x 1.5 x 0.5 in. targets. The targets were subjected to 1000°C in air for 4 hours using a Lindberg oven to sinter the pressed hydroxyapatite powder. The sintered targets were cooled to room temperature and attached to the face of a stainless steel 14 in. diameter water-cooled target using a high vacuum epoxy adhesive. The epoxy and was allowed to cure for 24 hours at room temperature and the hydroxyapatite covered target was placed into the vacuum chamber perpendicular to the ion beam for storage and use. Figure 3 displays a picture of the stainless steel target covered with hydroxyapatite tiles.

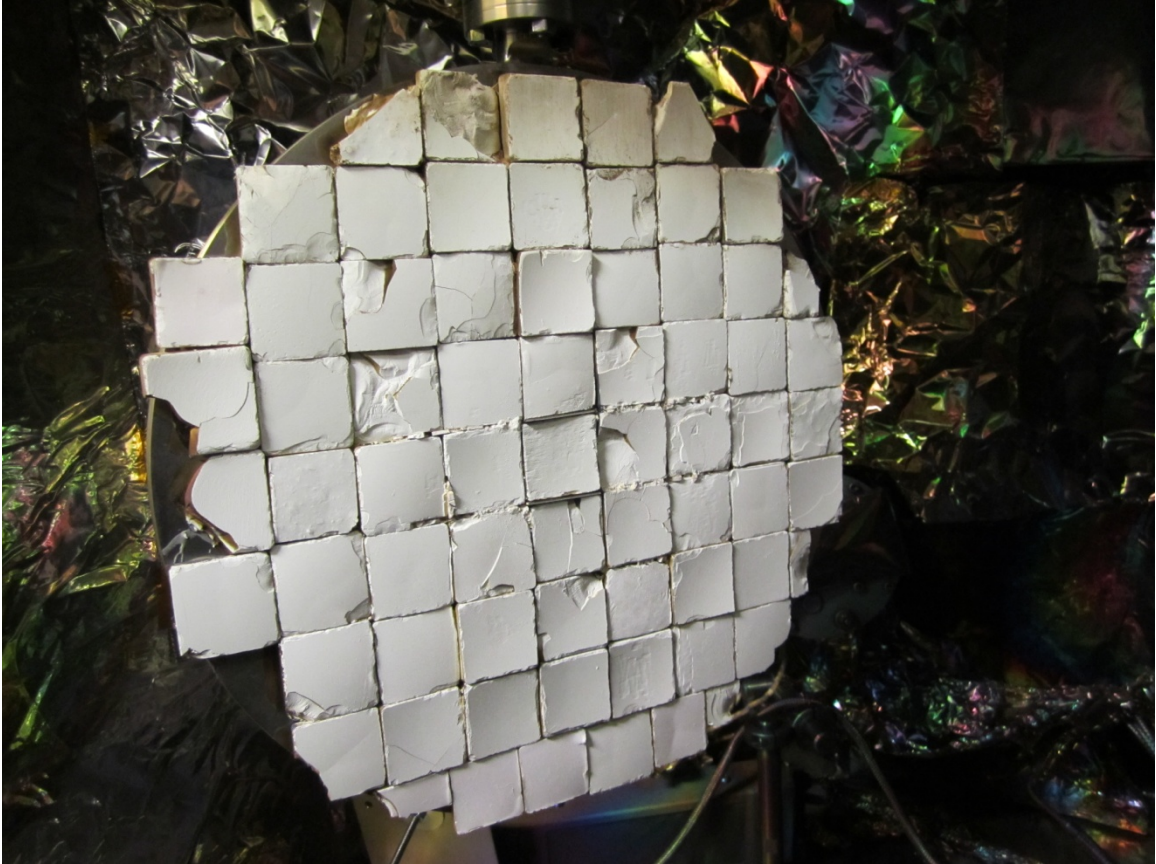


**Figure 3:** Sputtering target of sintered hydroxyapatite tiles

## 2.2: PLASMA REACTOR DESIGN AND DEVELOPMENT

The outside enclosure of the reactor was created using a 6 in. long 12 in. diameter stainless tube with a thickness of 0.025 in. Appropriate adjustments were made to the enclosure in order to accommodate the stand for the sample holder, thermocouples and electrical leads from the power supplies by cutting a 2 in. wide 4 in. long slot at the front of the enclosure. The 11in. diameter cylindrical anode was created from 0.010 gauge stainless steel shim stock and positioned in the enclosure with alumina stand-offs to isolate the anode from the enclosure and the rest of the vacuum chamber.

In order to increase the density of the plasma produced inside the reactor, the outside of the enclosure was spot welded with 1 in. wide 0.010 gauge steel shim stock strips positioned along the midline and rims of the enclosure. Magnets were oriented around the enclosure along the steel shim stock. The magnets along each rim of the enclosure were oriented with their north poles directed clockwise while the magnets along the midline were oriented with their north poles directed counterclockwise. Clear Teflon tubing was wrapped around the outside of the enclosure against the magnets to provide water cooling and prevent demagnetization of the magnets as the plasma source reached high temperatures.

The sample holder was created using a 2 ½ in. wide 4 in. long stainless steel plate and fashioned with a center bolt to attach to the stand as well as the electrical lead to the power supply. The sample holder was oriented vertically and positioned 2 inches behind the two tungsten filaments which were used to create the plasma discharge between the samples and the anode. The sample holder was isolated from the rest of the enclosure and vacuum chamber using an alumina ceramic standoff. Figure 4 displays photos of the completed plasma source setup. Initially heaters were installed in front of and behind the sample holder but these were later removed to incorporate a new design.

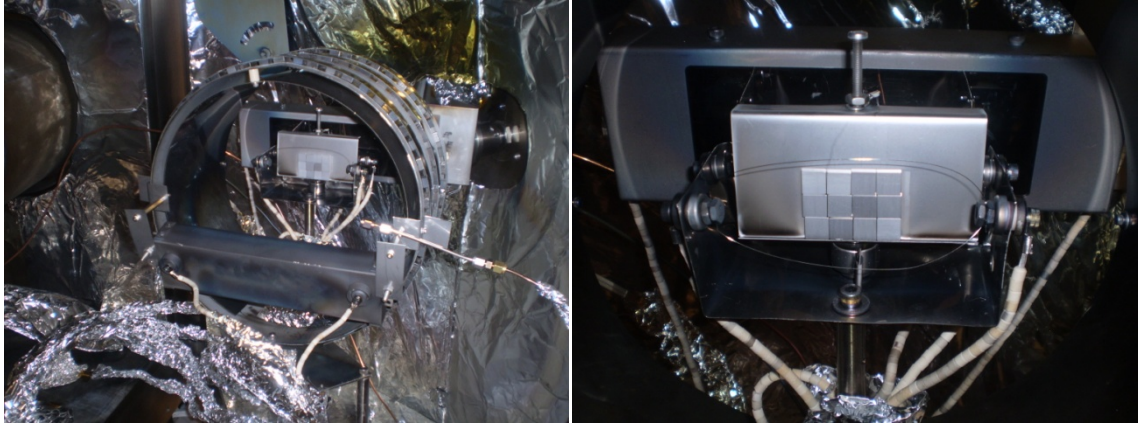


**Figure 4:** Plasma source assembly

### 2.3: PLASMA PRE-ETCH OF TITANIUM SUBSTRATES

For pre-etch processing of the substrates, the cleaned titanium samples were placed on the sample holder able to fit a maximum of 35 samples per run (5 rows with 7 samples per row). The four corner substrates and the middle substrate of each run were pre-weighed 3 times before the procedure and recorded. The vacuum chamber was pumped down to approximately  $1 \times 10^{-5}$  torr and backfilled with 50 sccm of Argon gas. The filament current was set to 12 to 13A with the discharge set to a voltage of 45V and a current between 4 to 5A. The sample holder was biased at a pulsing voltage of -700eV at a frequency of 1KHz and a duty cycle of 50%. The output current of plasma was maintained at approximately 120mA to 135mA. The samples were pulse biased at -700eV in the plasma for a prescribed period of time in order to etch to a depth of one micron and allowed to cool to room temperature in vacuum before venting the chamber.

After processing in vacuum, the same four corner substrates and the middle substrate were removed from the sample holder, post-weighed and recorded. Using the difference in the mass before and after plasma processing ( $\Delta m$ ) along with the density of pure titanium at near room temperature ( $\rho = 4.506 \text{ g/cm}^3$ ), the area of an individual sample

( $A=1\text{cm}^2$ ), and the change in time ( $\Delta t$ ), the etch rate for each titanium sample was determined in nm/hr using Equation 1:

**Equation 1**

$$\text{Etchrate (nm/hr)} = \frac{\Delta m}{\rho * A * \Delta t} * 10^7$$

In addition, using the formula used in Equation 1 and excluding the processing time ( $\Delta t$ ), the amount of material etched from each titanium sample was determined using Equation 2:

**Equation 2**

$$\text{Etchdepth (nm)} = \frac{\Delta m}{\rho * A} * 10^7$$

The -700eV pulse bias to the sample holder was controlled by a Spellman SL 600 high voltage power supply. The output pulse was to the sample holder was maintained using a fast switch which opened and closed at a frequency of 1 KHz with a duty cycle of 50% meaning the switch was on and off for equal amounts of time. The filaments were controlled by a Trygon Electronics 50-15 power supply and the plasma discharge connected to the anode which enclosed the sample holder was controlled by a Sorenson DCR 150-6B power supply. Figure5 displays an electrical schematic of the entire plasma source.

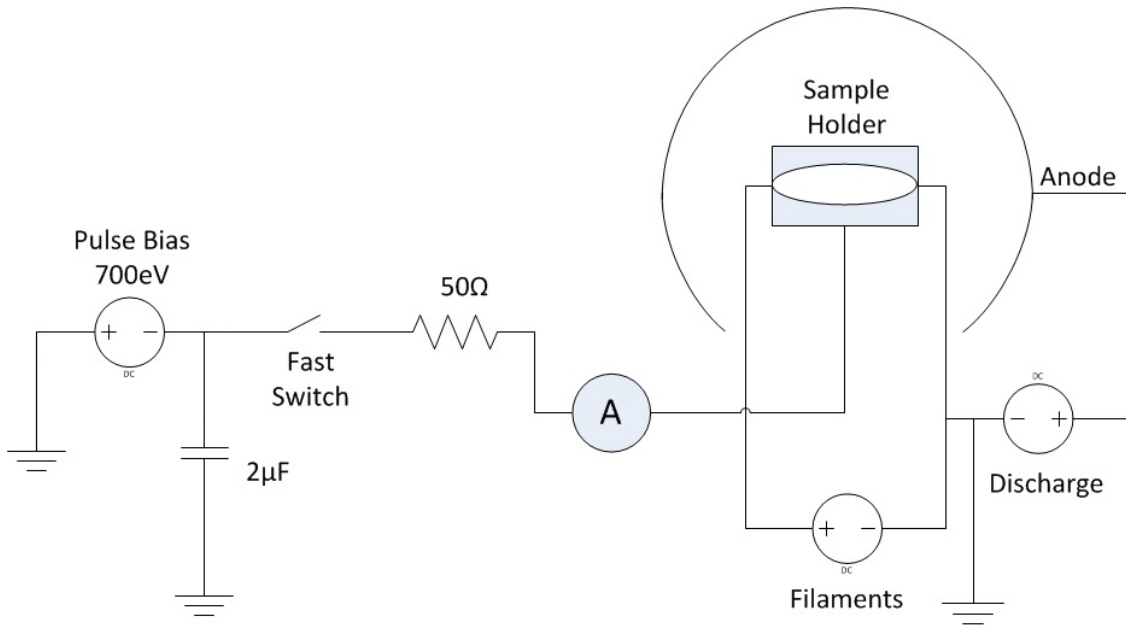


**Figure 5:** Wiring schematic of the plasma source

#### 2.4: ION BEAM SPUTTER DEPOSITION OF THIN FILMS

To sputter deposit the hydroxyapatite target and silver onto the titanium substrates, a 16 cm RF ion source was used. The substrates remained on the sample holder in the plasma source enclosure while the tungsten filaments used during plasma etching were removed and discarded. When sputtering hydroxyapatite only, the sputtering target was only covered with sintered hydroxyapatite tiles leaving no spaces between tiles for stainless steel to be accidentally sputtered into the film. When sputtering hydroxyapatite and silver, 0.010 in. thick silver strips were wedged between the tiles in the middle of the target. The chamber was pumped down to a pressure of  $1 \times 10^{-5}$  torr while the ion source was provided with 20 sccm of oxygen gas. The target was rotated 45 degrees from the ion source and in direct line of sight to the sample holder for uniform deposition across all of the titanium substrates.

As with the plasma etching procedures, the sample holder was able to hold a maximum of 35 samples per run for hydroxyapatite/silver sputter deposition. Three voltages were tested to determine the optimal sputter rate without creating damage to the hydroxyapatite tiles or the silver strips. The tested voltages were 300eV, 700eV, and 1100eV. During the preliminary tests, the higher voltages 700eV and 1100eV resulted in faster film deposition. However, 1100eV created excessive damage to the target such as loosening, cracking, and chipping of the tiles. It was determined that 700eV was the appropriate voltage to continue with all successive deposition runs. The beam current was set at a current of 300mA.

## CHAPTER 3: PHYSICAL AND MECHANICAL CHARACTERIZATION OF THE THIN FILMS

This chapter will discuss the methods, materials, results, and discussion of the all the tests used for physical and mechanical characterization of the thin films sputter coated on to the titanium substrates. The procedures used to characterize the films included contact profilometry, scanning electron microscopy, energy dispersive spectroscopy, adhesion testing using ASTM D3359-09 and stability testing using incubated PBS immersion.

### 3.1: METHODS AND MATERIALS

Since deposition time is dependent on the desired thickness of the film, contact profilometry was used to verify the surface profile. Previous studies on hydroxyapatite thin films in the Colorado State University Electric Propulsion and Plasma Engineering Lab has shown that ion beam sputtered hydroxyapatite thin films on etched titanium with a thickness of approximately 650nm are effective for mesenchymal stem cell proliferation and differentiation into osteoblasts [40]. Similarly, those films were also sputter deposited at a voltage of 700eV and it was determined that approximately 650nm could be achieved at 10 hours of ion beam deposition. The same procedure was followed in this study. Film thicknesses were verified through profilometry by sputtering hydroxyapatite thin films on a silicon wafer with a small fold of stainless steel foil covering a small section of the silicon substrate. When processing was complete after 10

hours, the foil was removed as well as the deposited film over the foil to reveal a completely coated silicon substrate except for the small section that was covered by the stainless steel foil. This allowed for a visible step between the bare substrate and the top of the film for the tip of the profilometer to detect. Film thickness was determined by dragging the tip across the silicon substrate and onto the coated regions. This process was completed for 3 different silicon samples to verify an average film thickness.

The topographies of the titanium substrates etched at 700eV were examined under high magnification using a field-emission scanning electron microscope (SEM, JEOL JSM 6500F). Substrates were examined using both low and high magnification to determine that the appropriate micro-scale and nano-scale features were present. These topographies were compared to etched titanium substrates from previous studies in our lab that have shown to produce micro-scale and nano-scale features advantageous for mesenchymal stem cell proliferation as well as osteoblast differentiation and proliferation. Those samples were etched using an ion source at a voltage of 700eV [40]. In addition, the topographies of etched titanium substrates with sputtered thin films of hydroxyapatite doped with silver were also examined using scanning electron microscopy and compared with plain un-etched titanium to determine the differences in surface structures and features. The surfaces of the substrates were imaged at a working distance of 10cm and a voltage of 15kV. Since hydroxyapatite is non-conductive, each substrate was sputter coated with 5nm of gold before viewing under the microscope to achieve adequate resolution. After gold coating, the substrates were attached to a conducting stub or microscope holder using small amount of double-sided carbon tape and grounded using graphite or copper tape. Two samples for each group were evaluated under SEM

(n=2). The amount of silver in the films were determined using energy dispersive x-ray spectroscopy (EDS) attached to the SEM (JEOL JSM 6500F). After obtaining an image of the substrate at 100x magnification, 3-5 different areas of the sample were subjected to EDS using the Spectrum feature on the EDS NSS analyzing software. Quantitative results were obtained for each area of the sample to determine weight percentage of each element present on the substrate. Silver concentrations for each area were recorded from the weight percentage (wt%) value and averaged to determine the total weight percent of silver in the sputtered thin film. In order to determine the equal distribution of silver over the entire area, the Spectral Imaging feature on the EDS NSS analyzing software was used. After obtaining an image of the substrate at 100x magnification, the Spectral Imaging feature was used to determine the location of each particle element in the film.

Two methods were used to determine the stability of the films on the titanium substrates: Adhesion testing by tape using ASTM Standard D3359-09 and long-term incubated phosphate-buffered saline (PBS) immersion. The former involves using ASTM Standard D3359-09 as a qualitative test which evaluates the adhesion of a film on a scale from 0B to 5B. A film classified as 0B on the scale corresponds to more than 65% of the film removed while a film classified as 5B corresponds to 0% of the film removed. This test provided a simple means to assess the quality of the mechanical interface between the film and the substrate. First, a razor blade was used to score a grid into the film with approximately 1mm spacing between each score (6 horizontal scores and 6 vertical scores). An appropriate length Nitto Denko/Permacel 99 polyester/fiber packaging tape was cut and adhered to the surface of the substrate for 90 seconds. After 90 seconds, the tape quickly removed by quickly pulling the tape across at a 180 degree angle without

jolting the tape or the substrate. The substrate and the tape were analyzed and compared to the ASTM Standard D3359-09 scale and classified from 0B to 5B. For each group containing a film coating, two substrates (n=2) were tested and compared to the standard.

The second of the two stability tests involved immersing the substrates in sterilized phosphate-buffered saline (PBS) in 37°C 5% CO<sub>2</sub> incubation for a prolonged period of time. The purpose of this study is to determine if the films are able to maintain a strong interface with the substrate in a static aqueous environment similar to *in-vivo* conditions. Five samples from each group (n=5), excluding plain titanium, were each weighed five times and carefully placed into a 24 well plate containing 1mL of PBS solution in each well. The substrates were incubated in the solution for a period of 4 weeks. At two weeks, the samples were evaluated visually to note any changes in color to the substrate or solution without removing the substrates from the PBS. After the 4 week period, the substrates were removed from the PBS solution, carefully rinsed with deionized water to remove any salt remnants, and weighed to determine any changes in mass. The PBS solutions from each well were carefully saved and stored for further evaluation.

### 3.2: RESULTS AND DISCUSSION

Contact profilometry revealed an average film thickness of 600nm across all three silicon samples. The profilometer was calibrated to zero microns across the silicon sample in order to obtain a measured value of the profile as the needle made contact with the top of the film. Figure 6 displays the measured surface profile across one of the tested silicon samples.

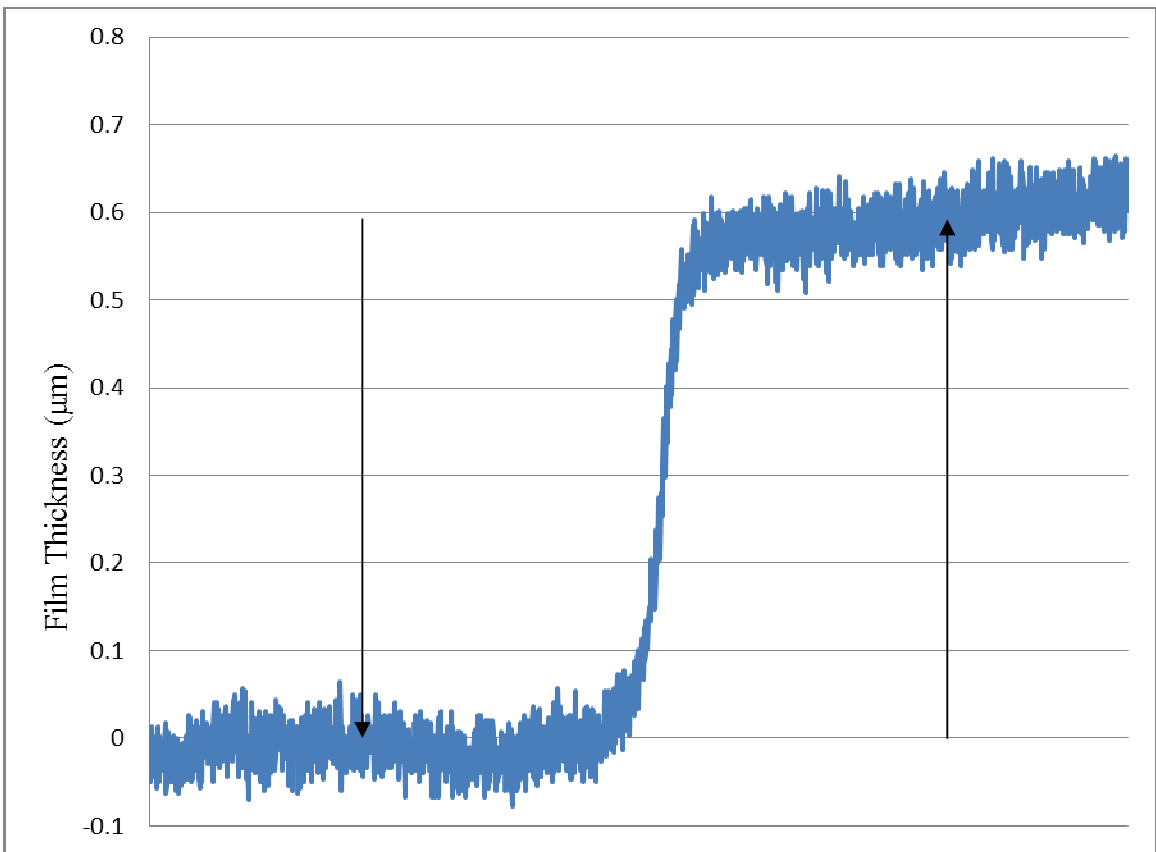


**Figure 6:** Surface profile of film thickness using contact profilometry

After etching the substrates at a pulsing voltage of -700eV in the plasma source for two hours and an etch depth of 1 micron, the SEM images displayed very unique micro-scale and nano-scale topographies. On the micro level, the collision cascade

created by ion bombardment in the plasma produced a random pattern of peaks and divots up to a few microns in size. On the nano level, it created step size features that are on the order of a few hundred nanometers. Figures 7 show the SEM images of the etched titanium samples at low and high magnifications to observe both the micro and nano-scale features. This textured surface closely mimics the structure of bone at the microscopic level which is advantageous for bone cell attachment and growth.

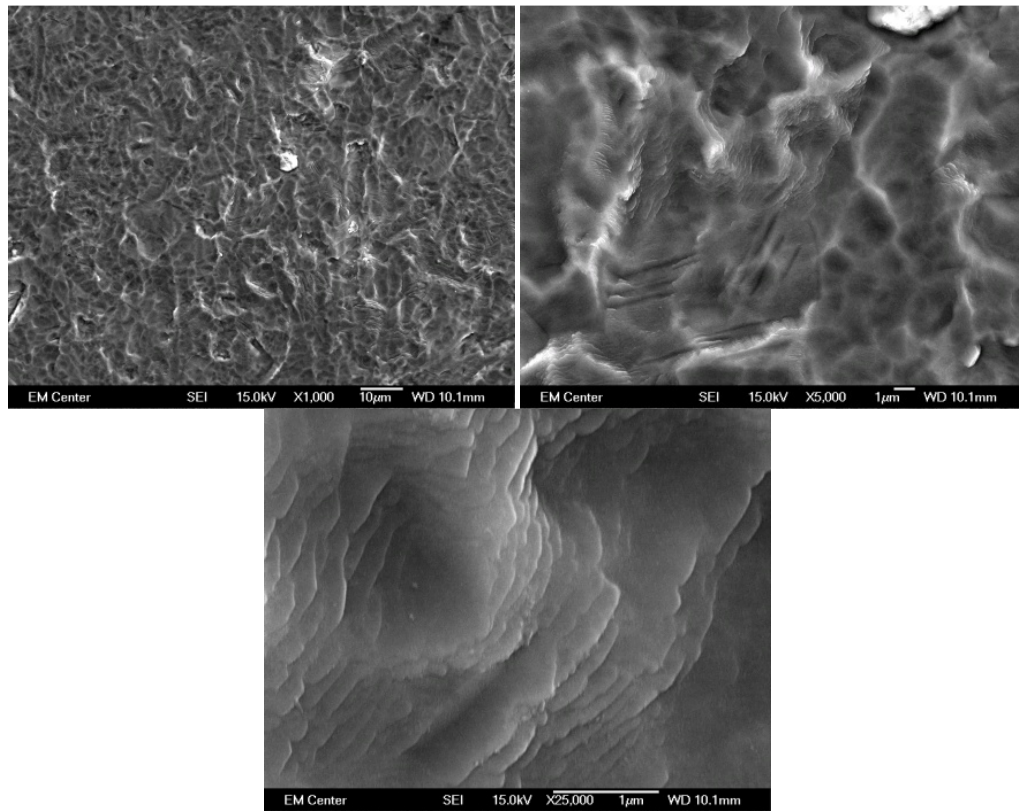


**Figure 7:** -700eV Etched Titanium Substrates at 1000x, 5000x and 25000x

When comparing the titanium etched for 2 hours at a pulsing voltage of -700eV in the plasma source to titanium etched for 15 hours at under at 700eV ion source, it was determined that the same topography was produced in the plasma source in a significantly shorter amount of time. Figure 8 displays side-by-side SEM images of samples etched using the two different processing methods. Figure 9 shows the

topographical differences between as received unmodified titanium and titanium etched at -700eV with a sputter coated thin film of hydroxyapatite doped with silver. Unlike the unmodified titanium, the sputter-coated etched titanium provides an evenly textured surface with a similar biochemistry to the bone matrix.

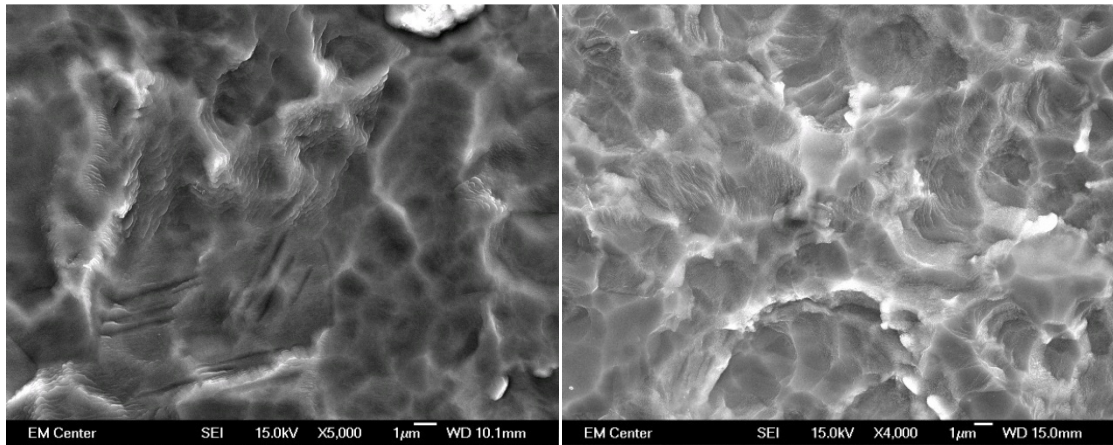


**Figure 8:** Micro-scale topography from plasma (left) and ion beam (right) processing

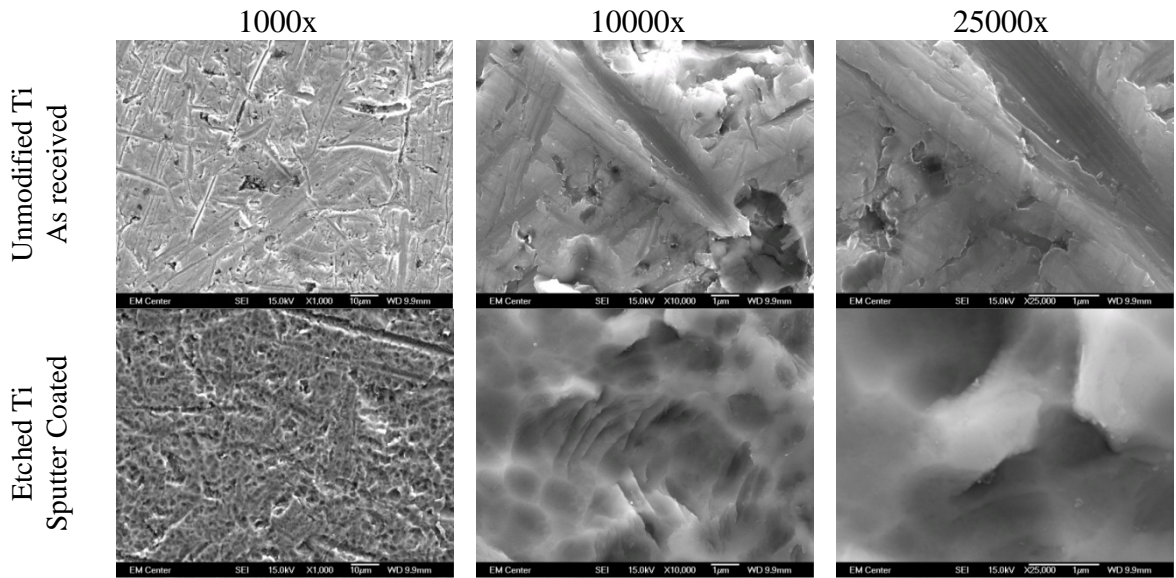


**Figure 9:** Comparison between unmodified Ti and etched Ti coated with HAp + Ag

Evaluation of plain titanium substrates under EDS revealed a spectrum containing over 99% titanium with trace amounts of carbon and vanadium. The Thermo Scientific periodic table for the EDS NSS analyzing software shows that vanadium peaks in the spectrum are often associated with titanium. Evaluation of the etched titanium substrates coated with hydroxyapatite only thin films revealed peaks corresponding to calcium, phosphorus, oxygen, titanium and minimal amounts of carbon and vanadium. For the titanium substrates coated with hydroxyapatite doped with silver, EDS was primarily used to determine the wt% of silver in the film using the quantitative results of the spectrum. As previously stated, the first test group of substrates contained a lower concentration of silver in the film (A1) and the second test group of substrates contained a higher concentration of silver in the film (A2). The targeted weight percentages initially were 0.5wt% and 1.0wt%. Final average values of the tested areas revealed that the concentration on the low silver substrates was  $0.63 \text{ wt}\% \pm 0.29$  and the concentration on the high silver substrates was  $1.53 \text{ wt}\% \pm 0.33$  which are slightly higher than the goal percentages but still within reasonable range (Figure 10). EDS results from spectral imaging at 100x magnification determined equal distribution of calcium, phosphorus and silver across the films for both the A1 group and the A2 group (Figure 11).

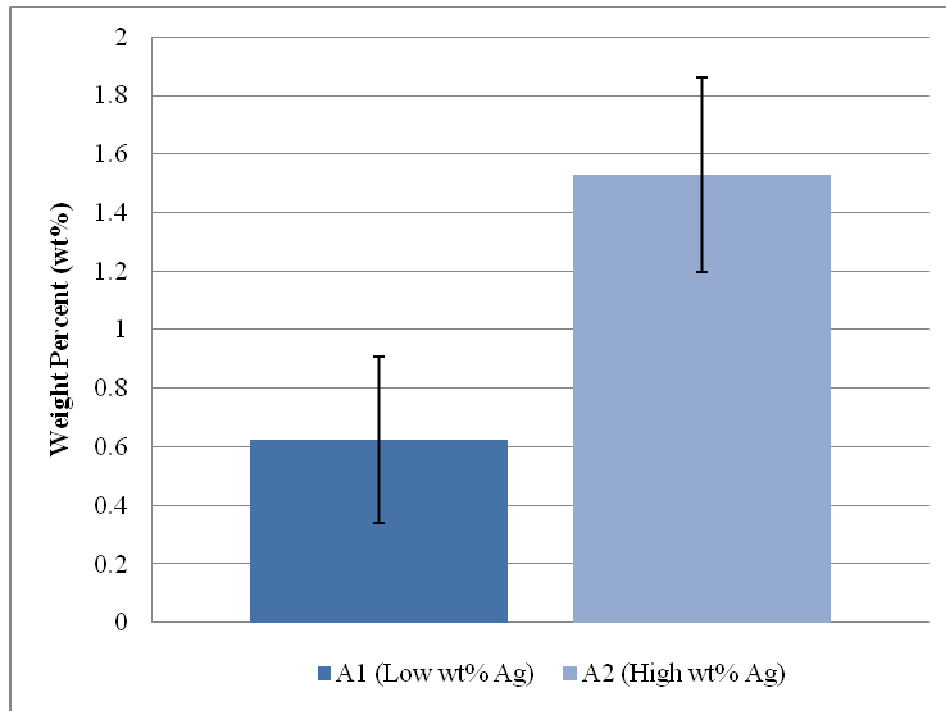


**Figure 10:** Weight percentages of silver in the hydroxyapatite films

**A1:** Hydroxyapatite + Low wt% Ag

**A2:** Hydroxyapatite + High wt% Ag

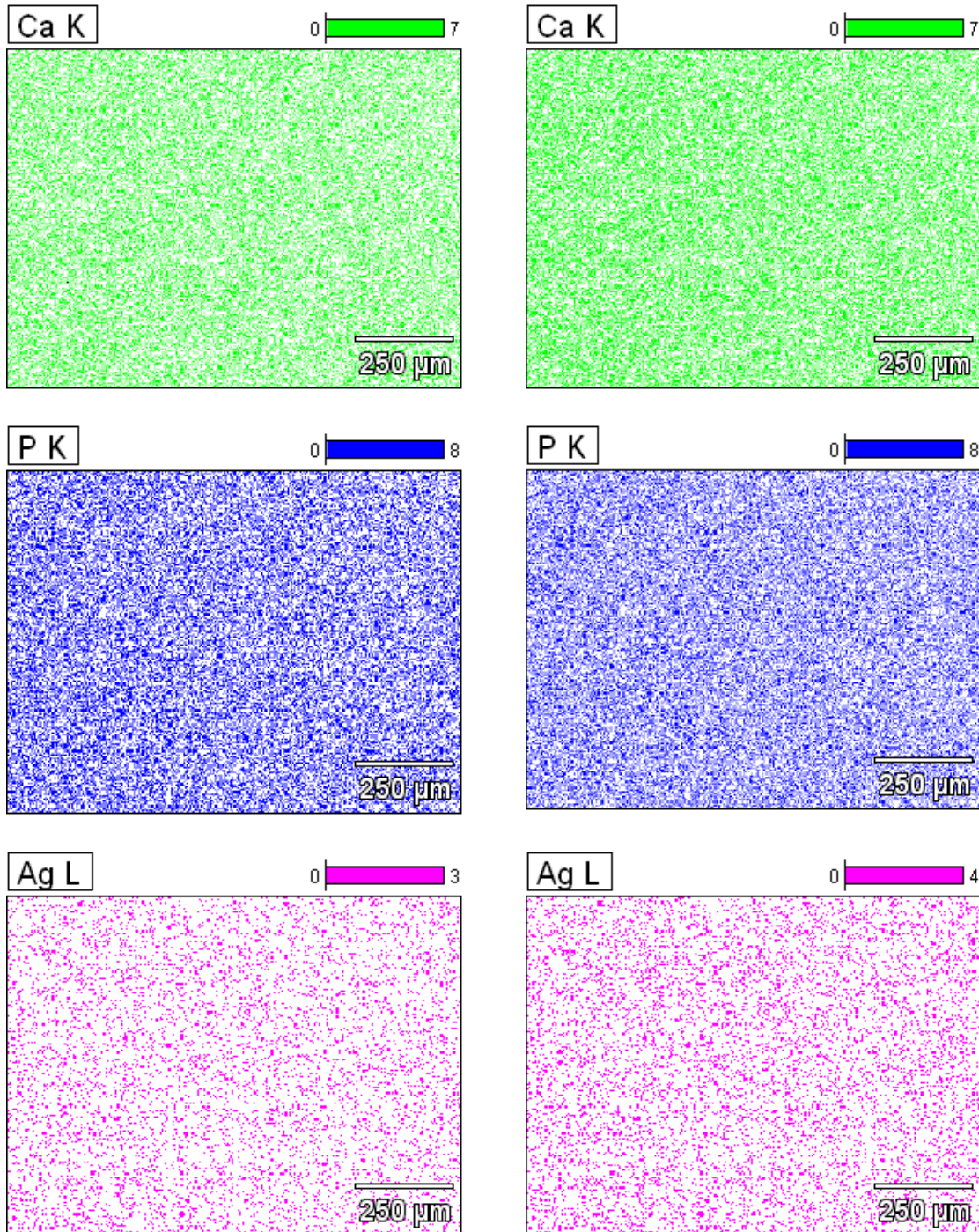


**Figure 11:** Spectral imaging of substrate groups A1 and A2

Film adhesion testing via ASTM Standard D3359-09 tape test was used to evaluate 3 different substrates from each of the coated groups (H, A1, and A2). The results revealed that on all substrates, there was no delamination or disturbance of the films. This indicated that all tested substrates were classified according to the standard as 5B (0% of the film removed). The results also signify that the mechanical interface between the film and the etched titanium substrate is strong enough to withstand mild to moderate forces of destabilization.

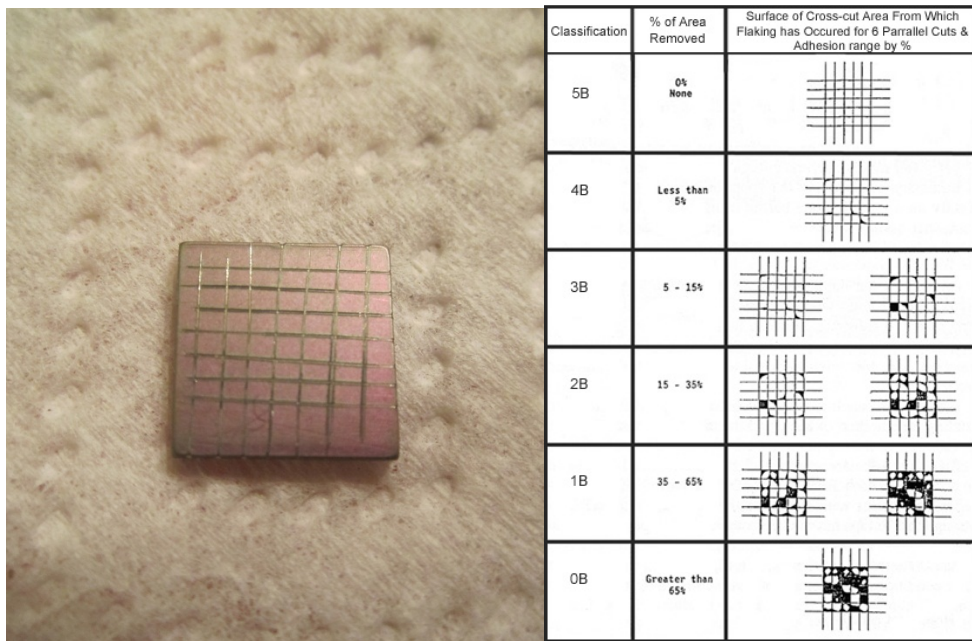


**Figure 12:** ASTM D3359 Adhesion by Tape Test

The results of the long-term stability using incubated PBS immersion revealed very different results. Before the substrates are subjected to the study, it is noticeable to report that the color of the coated samples in comparison with plain titanium. The coated samples have a very unique teal or maroon appearance depending on the amount of light in the room and the viewing angle. During PBS immersion, it was discovered at 2 weeks through visual observations that the color of the substrates was beginning to change and

fade from teal/maroon to grey indicating that the film was either dissolving in the solution or was delaminating from the surface. After the 4 week prescribed period in 37°C 5% CO<sub>2</sub> incubation, the substrates removed from the PBS solution and gently rinsed with deionized water had shown no significant decrease in mass. Even though the scale was able to read to the nearest hundred thousandth value, the average mass change for all the samples was less 0.00002 grams. The 1mL PBS solutions in the 24 well plates were allowed to completely evaporate in the well plates to reveal visible delaminated films left behind from the substrates along with traces of salt from the PBS solution. In some cases, the large sections of the films remained intact as very thin and fragile sheets. Figure 13, shows pieces of translucent thin films delaminated and left behind after PBS evaporation in the well.

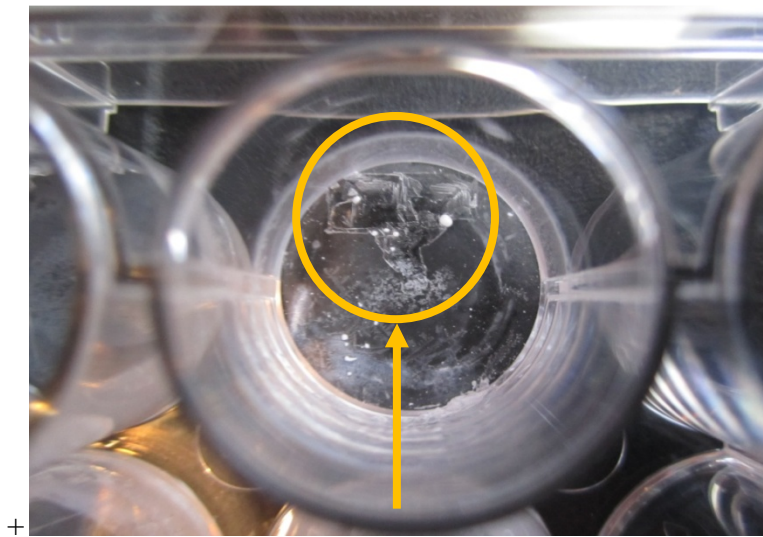


**Figure 13:** Delaminated films after PBS immersion for 4 weeks

To further assess the delamination of the films from the stability study, one sample from each of the coated groups (H, A1, and A2) was examined under SEM and analyzed using EDS. SEM images of each substrate visibly revealed large noticeable

areas of the where the film had been attached leaving behind small remains of the film that managed to stay mechanically bonded to the etched titanium.

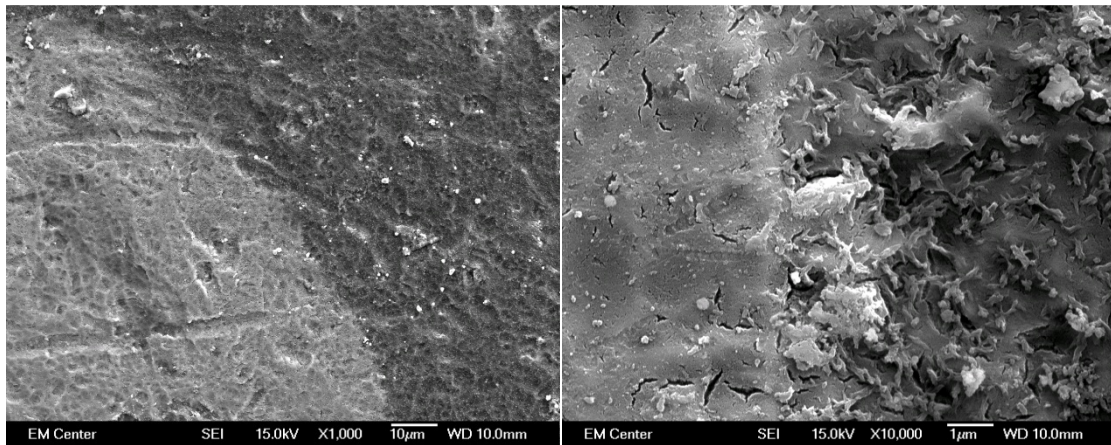


**Figure 14:** Film Delamination at 1000x and 10000x

Quantitative results for the EDS scans displayed a significant drop in the weight percentage of silver left on the titanium substrates. Before the stability study, the concentrations of silver in the films were 0.63 wt% and 1.53 wt% respectively for groups A1 and A2. After the stability study, the concentrations of silver in the films were 0.15 wt% and 0.27 wt% respectively for groups A1 and A2 due to excessive delamination. The average results from EDS values before and after are shown in Figure 15.

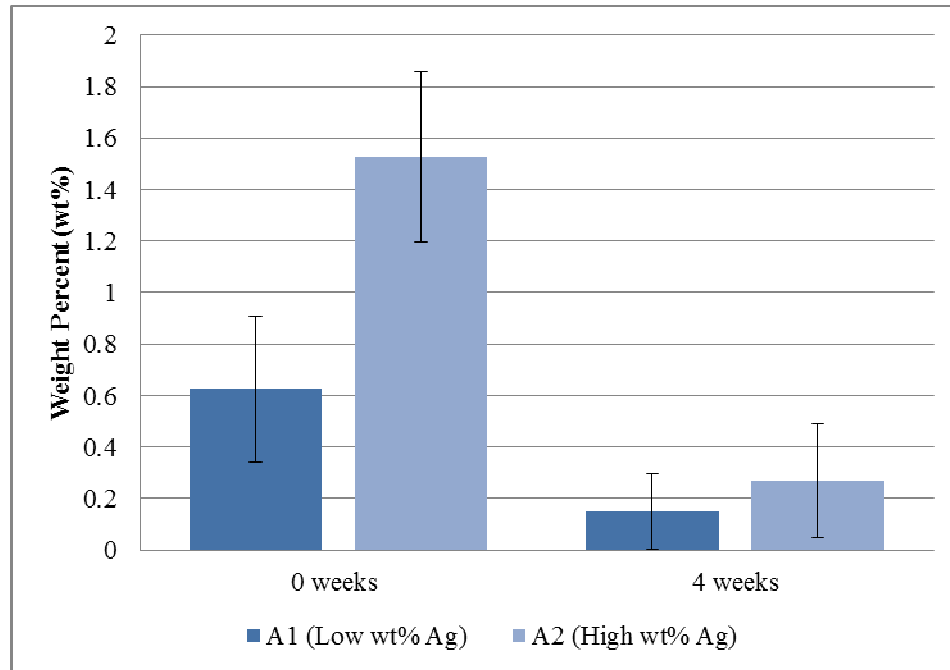


**Figure 15:** Evaluation of silver wt% before and after stability studies

Since the films did not begin to display significant signs of degradation or delamination within the first week of the stability study, it was decided that the project would move forward with the bacteria studies since the goal was to look at the short-term initial response from the bacteria regarding their interaction with the doped silver particles in the films. Judging from the positive results received from tape testing, it was presumed that the films would be able to uphold their strength and mechanical bond to the titanium substrates during the short-term bacteria adhesion studies.

## CHAPTER 4: BACTERIAL RESPONSE OF SILVER-DOPED HYDROXYAPATITE THIN FILMS

The following chapter will provide an overview of the methods, materials, results, and discussion regarding the bacterial studies that were conducted on the processed substrates. In all, two studies were performed using aerobic bacteria strains commonly found in orthopedic infections in order to investigate bacterial adhesion and bacterial response to silver particles released into suspension from delaminated films.

### 4.1: METHODS AND MATERIALS

The aerobic gram positive bacteria strain used in the study was *Staphylococcus epidermidis* (*SE*, RP62A) and the aerobic gram negative strain used in this study was *Pseudomonas aeruginosa* (*PA*, PA01). For adhesion studies, the substrates were placed in triplicate into sterilized 12 well plates (one 12 well plate per bacteria strain for each group: T, H, A1, and A2). The samples were carefully cleaned and sterilized with ethanol and subjected to ultraviolet (UV) light in a biosafety cabinet. Both cultures of *SE* and *PA* were adjusted overnight to a concentration of  $5 \times 10^4$  cells/mL in fresh Tryptic Soy Broth (TSB) medium and 3mL of  $10\text{g/L}$  were added to each well. After seeding bacteria on onto the substrates, the plates were incubated at  $37^\circ\text{C}$  on a shaking plate at 125 RPM. Each plate was placed in the incubator shaker for 5 minutes to disperse the bacteria in the medium before  $T$  (time) = 0.

The bacteria were allowed to adhere to the substrates for time points of 8 hours, 24 hours, 32 hours, and 48 hours. Media changes occurred at 24 and 32 hours. At each time point the bacteria were stained with Live/Dead BacLight™ (Invitrogen) stains and counted microscopically. The Live/Dead stain contains SYTO 9 which cause living bacteria cells to fluoresce green and propidium iodide which causes dead bacteria cells to fluoresce red. The propidium iodide is unable to penetrate cell membranes which are still intact so living cells will reject this dye. However when a dying bacteria cell is no longer able to maintain its membrane, the propidium iodide is able to enter the cell and interact with the DNA of the cells. The grid area or picture area was  $2 \times 10^{-8} \text{ m}^2$ , the filter membrane area was  $0.0002 \text{ m}^2$ , and the sample volume for each count was 1mL. For each substrate, live cell counts and dead cell counts were each taken 5 times and averaged. Dilution factors for each sample were based on the final volume divided by the aliquot volume. In order to determine the concentration of live bacteria and dead bacteria per samples, Equation 3 was used. Once the bacteria concentration values were calculated for all of the samples, the concentrations were averaged for each of the time periods: 8 hours, 24hours, 32 hours, and 48 hours. At time 8 hours and 32 hours, the adhered bacteria were fixed to the substrates for SEM imaging with 3% glutaraldehyde and dehydrated with a series of ethanol baths.

### Equation 3

$$BacteriaConcentration (cells/cm2) = \frac{C * M * DF}{G * V} * 1.5/1$$

C: Average of # of live or dead cells (cells)  
M: Filter membrane area ( $\text{m}^2$ )  
DF: Dilution Factor (unitless)  
G: Grid Area ( $\text{m}^2$ )  
V: Sample Volume (mL)

In addition to the bacteria adhesion study, a film release study, similar to a drug release study, had to be conducted. Contrary to initial assumptions, the films were beginning to delaminate in TSB media after the samples were seeded with bacteria. It was discovered after that the samples were beginning to change color after the 12 well plates containing the samples, media, and bacteria were subjected to shaking incubation at 125 RPM. A similar protocol to the adhesion study was utilized for the release study. Substrates were placed in triplicate in sterilized 12 well plates with one plate per bacteria strain for each group: T, H, A1, and A2. The samples were carefully cleaned and sterilized with ethanol and subjected to ultraviolet (UV) light in a biosafety cabinet. Both cultures of *SE* and *PA* were adjusted overnight to a concentration of  $5 \times 10^4$  cells/mL in fresh Tryptic Soy Broth (TSB) medium and 3mL of 10g/L were added to each well. Once again, after seeding bacteria on onto the substrates, the plates were incubated at 37°C on a shaking plate at 125 RPM for 5 minutes to disperse the bacteria. For each hour, from 0-8 hours, aliquots of the medium were removed at filtered through a 100nm membrane. The trapped bacteria were stained with Live/Dead BacLight™ (Invitrogen) stains and counted using ImageJ software. Unlike the bacterial adhesion studies, only the viable bacteria cells (colony forming units) were counted. The cell counts were averaged at each time point and multiplied by the dilution to obtain the number of cells per milliliter.

## 4.2: RESULTS AND DISCUSSION

The concentration of dead Gram positive *Staphylococcus epidermidis* (*SE*) bacteria cells (Figure 16) observed on the four sample types at 8 hours showed that there was slightly more dead cells on the samples with films containing silver. At 24 hours, the number of dead bacteria cells considerably increased on the substrates with a high wt% of silver and continued to increase up to 48 hours. However, there was little difference between the 4 groups at 48 hours. It is presumed that the films had completely delaminated from the titanium substrates after two days in TSB media. When observing the number of live *SE* cells on the materials, there are a slightly lower number of cells at 8 hours and 24 hours on the substrates with a high wt% of silver. However this trend does not continue approaching 48 hours and there is no significant difference between the four groups (Figure 17).

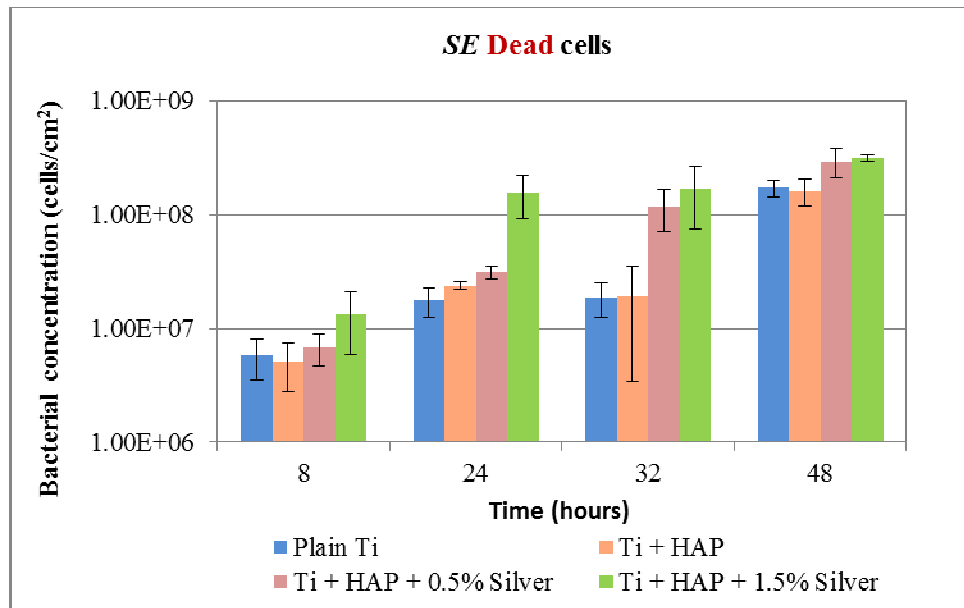


**Figure 16:** Bacteria adhesion of *SE*: Dead cells

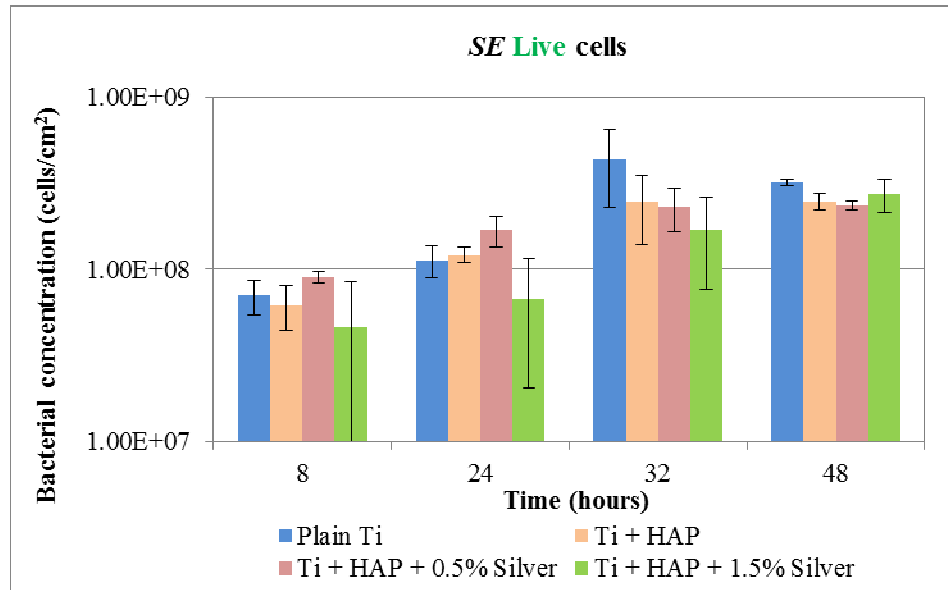


**Figure 17:** Bacteria adhesion of *SE*: Live cells

Observing the percentage of dead cells on the substrates may be more useful than looking at the bacterial concentration of cells because the percentage is irrespective of the number of cells present on the substrates. Instead, examining the percentage is helpful because it takes whatever number of cells and looks at whether there are more dead cells than live cells. At 8 hours and particularly at 24 hours, there is a significant higher percentage of dead bacteria on the on the substrates with high wt% of silver in comparison with the other groups. At 32 hours and 48 hours, the percentage of dead *SE* cells on the substrate with low wt% silver begins to increase while the control samples remain low (Figure 18).

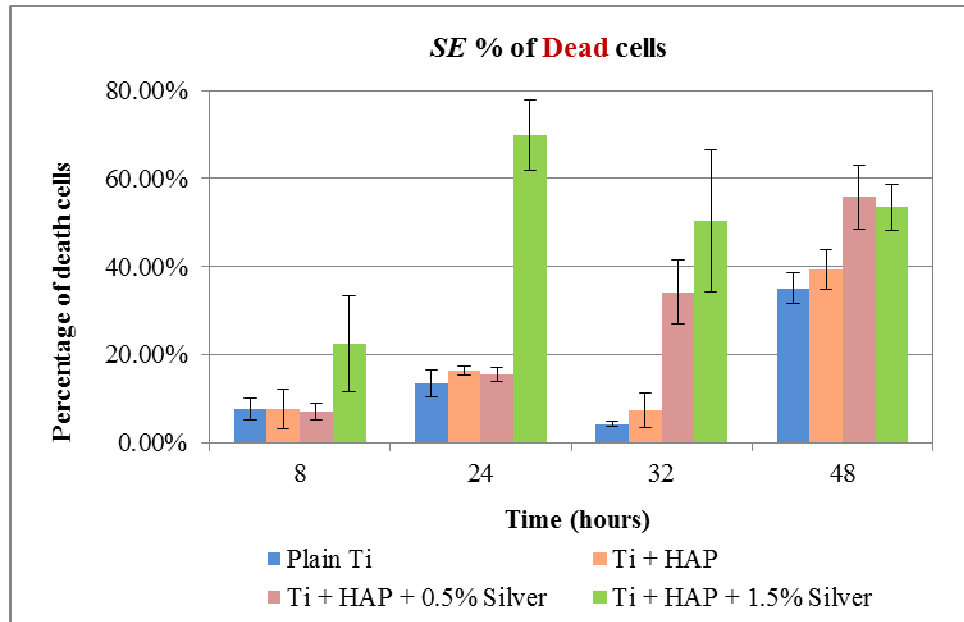


**Figure 18:** Bacterial adhesion of *SE*: % of Dead cells

The bacteria adhesion results for Gram negative *Pseudomonas aeruginosa* (*PA*) differed significantly from the *SE* observations. When evaluating the number of dead *PA* cells on the substrates (Figure 19), there were less dead cells on the substrates with silver present in the films at both 8 hours and 24 hours. At 32 hours and 48 hours, there was no considerable difference between each group even though the number of dead cells had increased for the substrates with silver. A similar trend seemed to occur when observing the number of live *PA* cells on the substrates (Figure 20). At both 8 hours and 24 hours, there was significant difference between the control groups and the groups with films containing silver. The samples with silver had a lower number of live cells but once again there was no significant difference after 24 hours. One very likely reason for this occurrence could be that the substrates sputtered with silver-doped hydroxyapatite had

immediately delaminated in the media after the bacteria was seeded. This could explain why the results showed both a lower number of dead and live cells on the substrates.

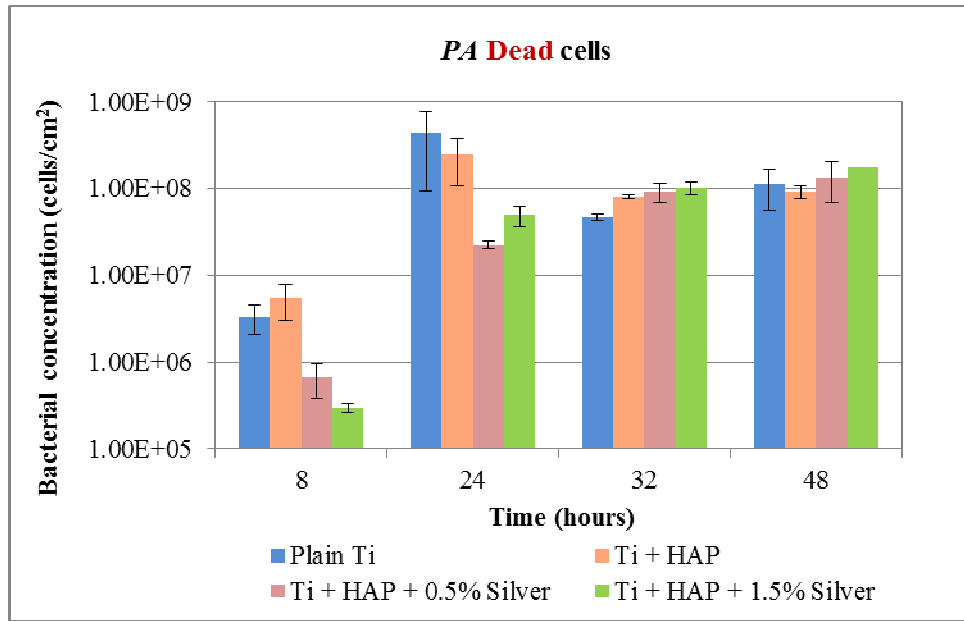


**Figure 19:** Bacterial adhesion of *PA*: Dead cells

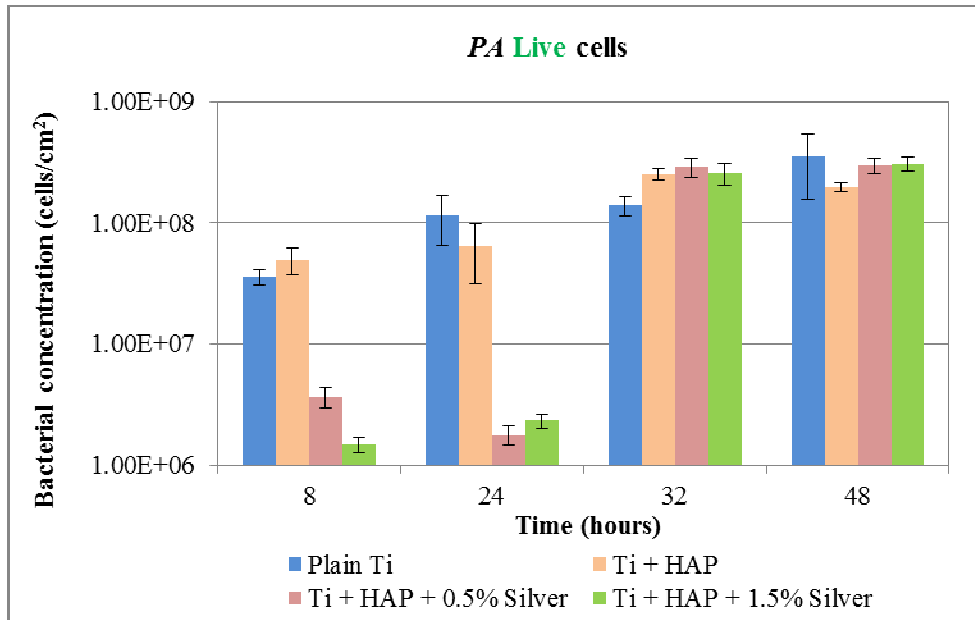


**Figure 20:** Bacterial adhesion of *PA*: Live cells

Once again, the percentage of dead cells on the substrates is important to look at because it doesn't matter how many cells present (Figure 21). The key aspect is determining if there are more dead bacteria than live bacteria. The results are very interesting because although there is a large spike in the percentage of dead cells across all sample groups, none of the groups are significantly different from one another when looking at each individual time point. These results further support the presumption that the films had delaminated early in the study. Otherwise, it would be expected that there would be a higher percentage of dead cells on the substrates containing silver in comparison with the control groups.

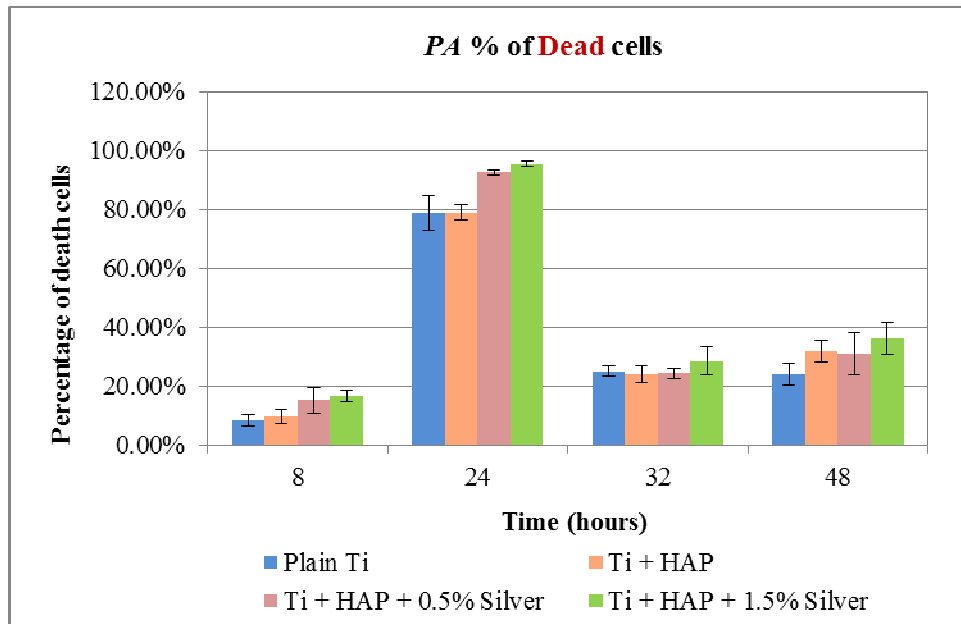


**Figure 21:** Bacterial adhesion of *PA*: % of Dead cells

Since the results from the bacteria adhesion studies are very inconclusive for both strains of bacteria, the SEM images of the fixed cells are very important. The images not only help determine the general behavior of the bacteria, it can also be used to determine the behavior of the films. Figures 22 and 23 display SEM images of bacteria cells on the control groups: T and H.

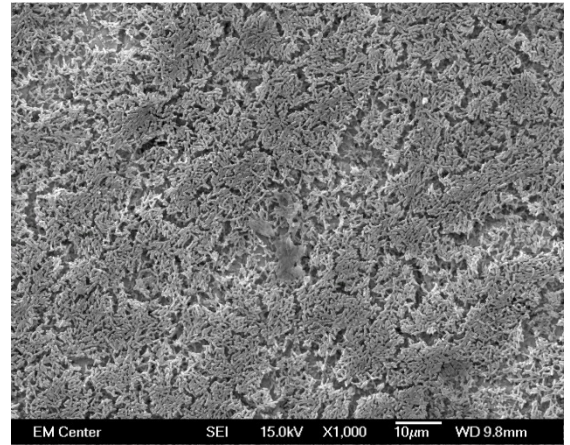
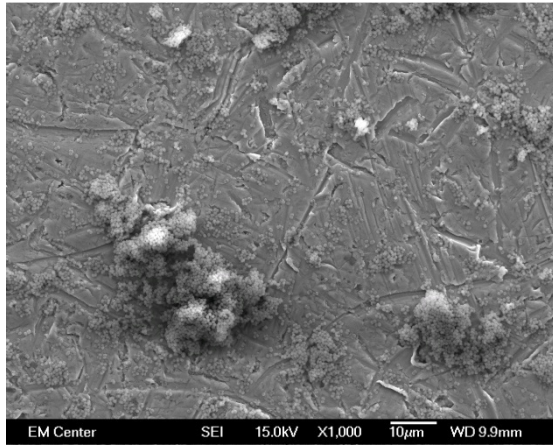
On plain titanium, it is expected that the many bacteria would adhere to the surface, form colonies, and eventually begin to deposit a biofilm. *SE* cells had formed massive colonies on the plain titanium that were spread across the substrate. Some of the colonies were so three dimensional that it was difficult to obtain an adequate image due to differences in contrast. As shown in the second image at 5000x magnification, the top bacteria cells were in the early stages of forming a biofilm around the colony. *PA* cells displayed far more drastic behavior on the plain titanium. As shown in the image at 1000x magnification, cells had completely covered the substrate. Although the *PA* cells did not form large three dimensional colonies like the gram positive bacteria, biofilms were very noticeable across the substrate.

On etched titanium coated with hydroxyapatite, it is expected that the bacteria would behave in a similar manner to the bacteria on titanium and that certainly was the case. *SE* cells had formed large three dimensional colonies and many of them were in the early stages of biofilm formation as shown in the images at 5000x magnification. Like plain titanium, the hydroxyapatite was completely covered in *PA* cells and very large biofilms were present across the substrate. However, some small areas near the edges of the substrate had little amounts of bacteria which are possible due to film damage.

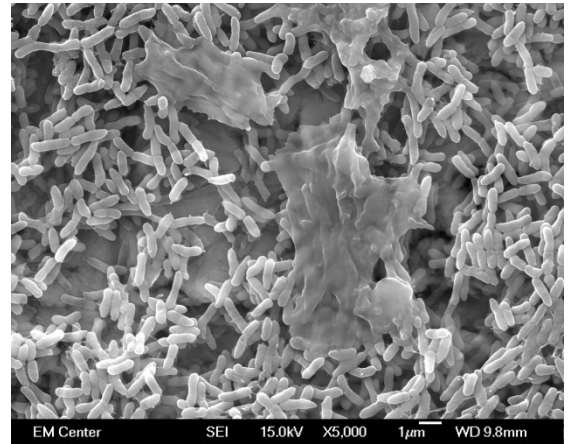
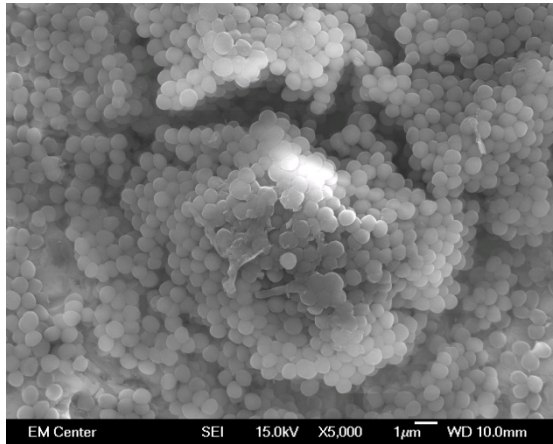
*Staphylococcus epidermidis*

*Pseudomonas aeruginosa*

1000x



5000x



5000x

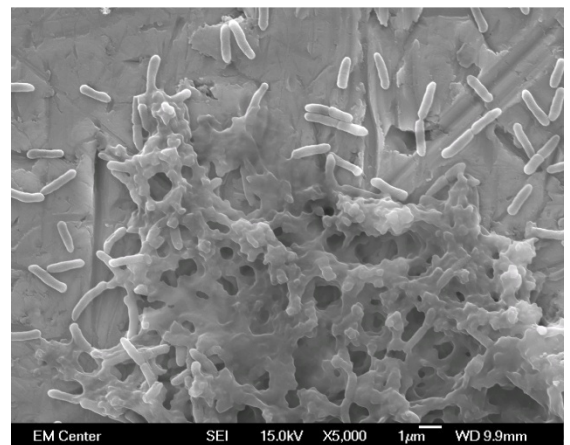
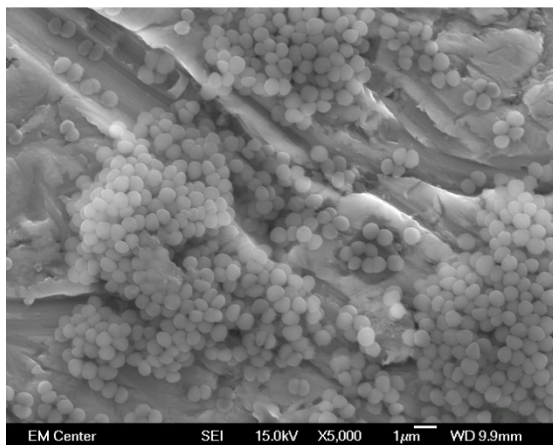
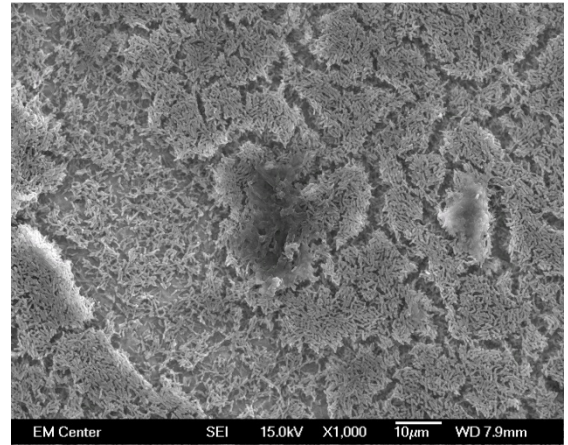


**Figure 22:** SE and PA cells on plain titanium

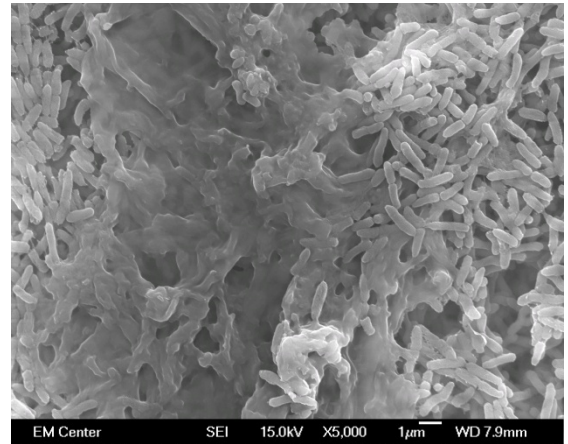
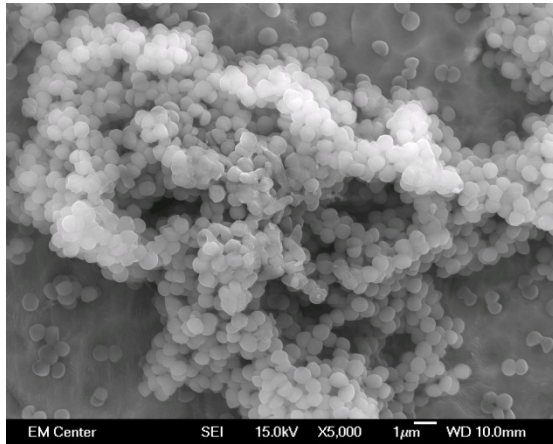
*Staphylococcus epidermidis*

*Pseudomonas aeruginosa*

1000x



5000x



5000x

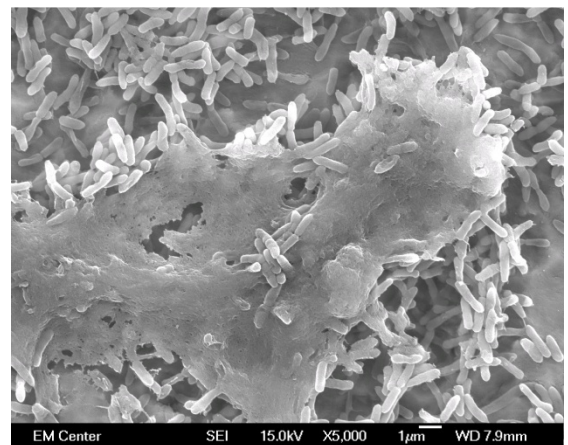
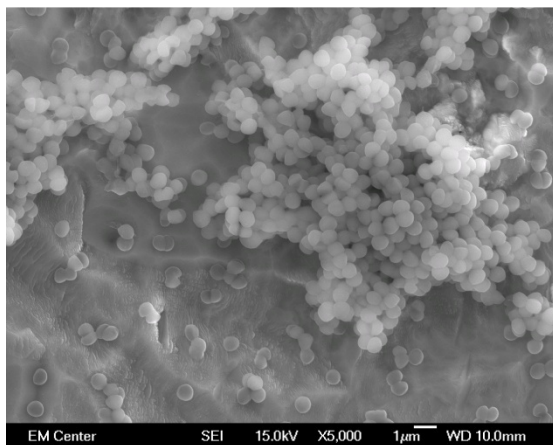


**Figure 23:** *SE* and *PA* on etched titanium coated with HAP

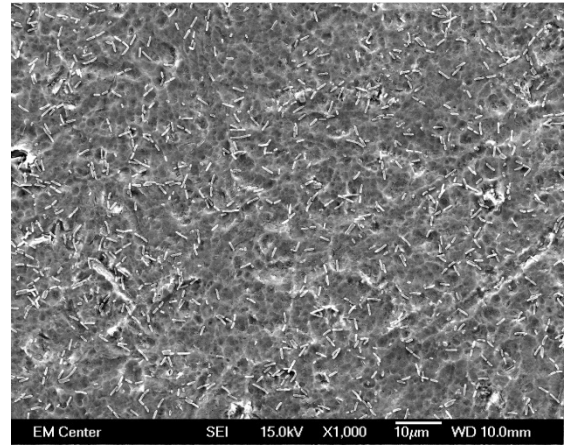
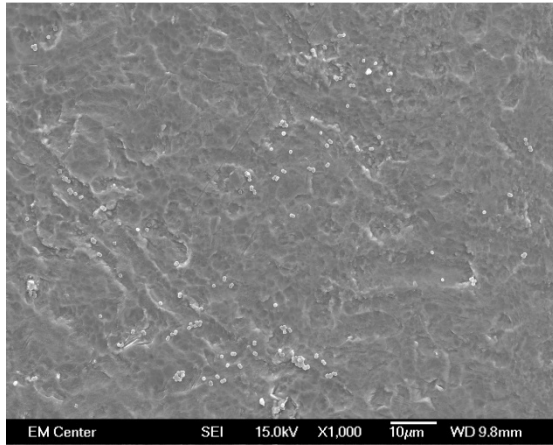
Figure 24 shows the SEM images of both bacteria strains on etched titanium coated with hydroxyapatite and a low wt% of silver. The expectation on this substrate group is that there would be fewer bacteria present due to the doped silver particles killing the bacteria and causing them not to adhere. As seen in the image at 1000x for both the *SE* and *PA* cells, there are far fewer bacteria on the substrate in comparison with the control groups. The *SE* cells had not formed large three dimensional colonies and any small colonies that were present on the substrate did not show signs of biofilm formation. The *PA* cells did not cover the substrate as they did on the control groups, however various areas did have some large colonies form with very small biofilms. It is likely that these colonies formed on sections of the substrate where delamination may have occurred.

Figure 25 shows the SEM images of both bacteria strains on etched titanium coated with hydroxyapatite and a high wt% of silver. Since the low wt% of silver substrates had fewer bacteria than the controls it is expected that the high wt% of silver substrates would be similar or better. It is noticeable on the images at 1000x magnification that there are very few bacteria present on the substrates. Similarly to the low wt% silver substrates, the *SE* cells had only small colonies and these colonies did not begin forming any biofilms. The number of *PA* cells was low across the surface, however in particular areas there were small colonies of *PA* cells present which had started forming biofilms. As with the other coated substrates, it is likely that these are areas where the film was damaged or beginning to delaminate therefore exposing the titanium surface.

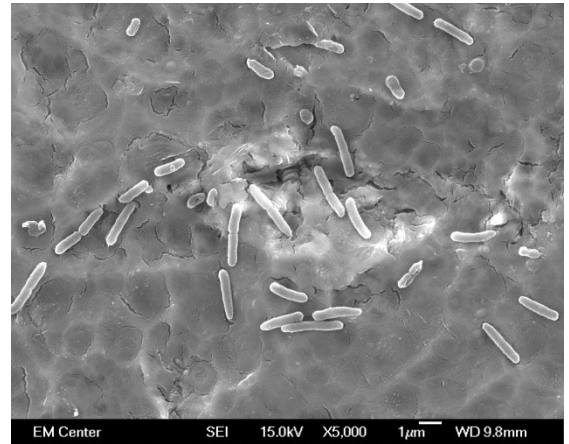
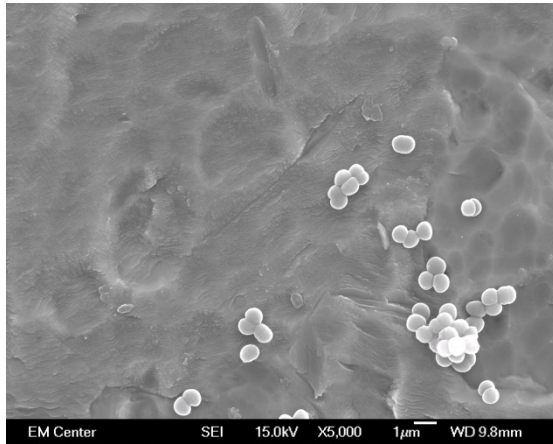
*Staphylococcus epidermidis*

*Pseudomonas aeruginosa*

1000x



5000x



5000x

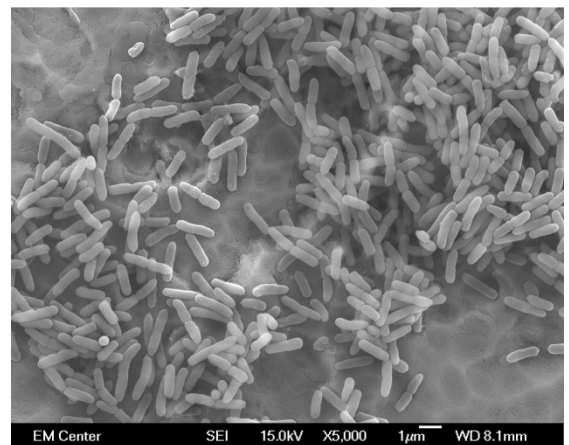
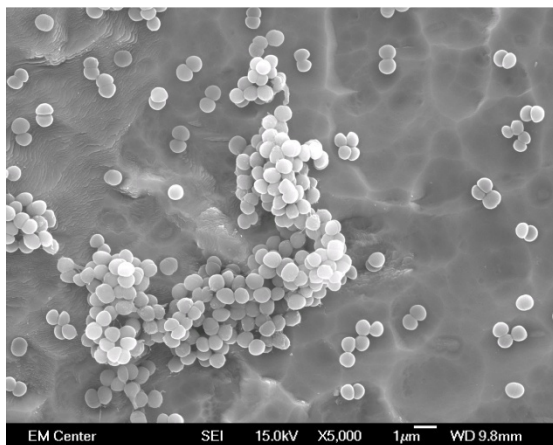
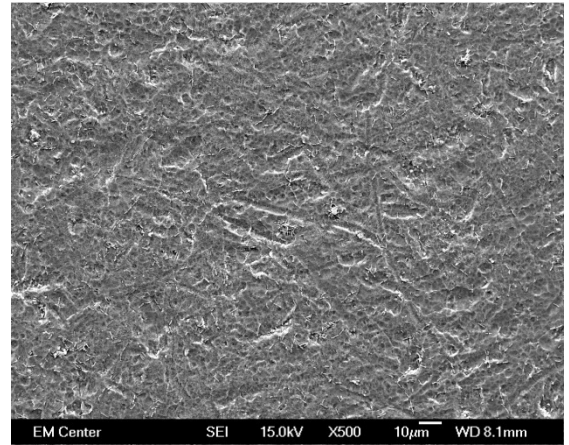
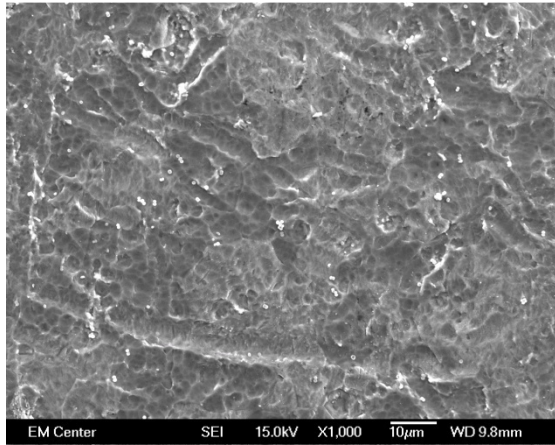


**Figure 24:** SE and PA on etched titanium coated with 0.5% silver-doped HAp

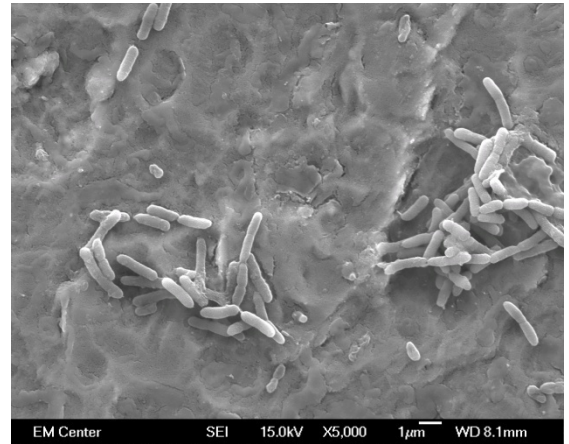
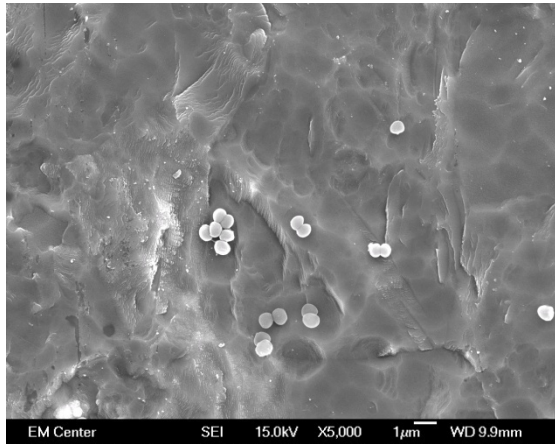
*Staphylococcus epidermidis*

*Pseudomonas aeruginosa*

1000x



5000x



5000x

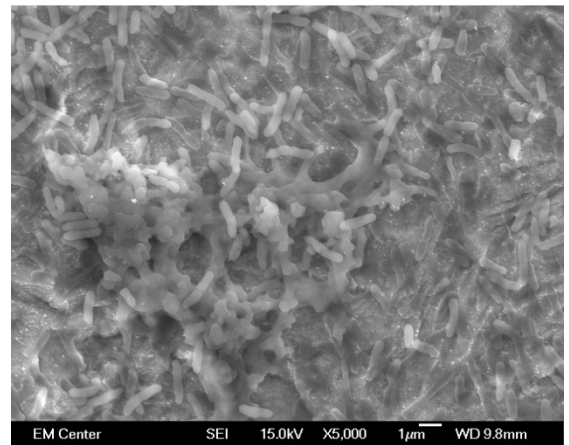
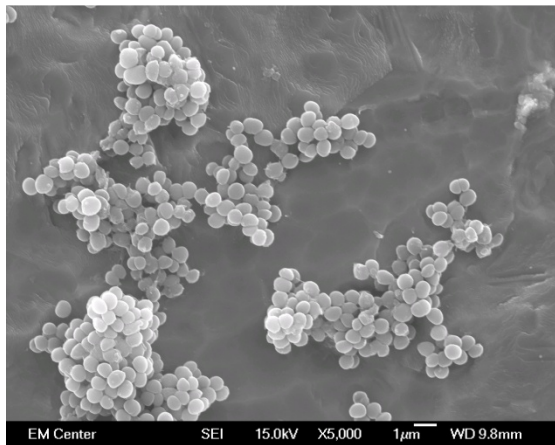


**Figure 25:** *SE* and *PA* on etched titanium coated with 1.5% silver-doped HAp

The release study delivered very promising results regarding the behavior of bacteria in suspension. Since the substrates had shown obvious signs of delamination it was important to determine if the silver was indeed killing the bacteria and reducing cell growth. Figure 26 shows the growth of *SE* cells over 8 hours in suspension with the four substrate groups. Noticeably, the control groups displayed significant bacteria growth with slight cell death occurring between 6 and 7 hours with titanium. The substrates with silver displayed no *SE* cell growth until 5 hours when the growth began to slowly increase. As expected, the higher silver concentration performed the best in preventing bacteria growth.

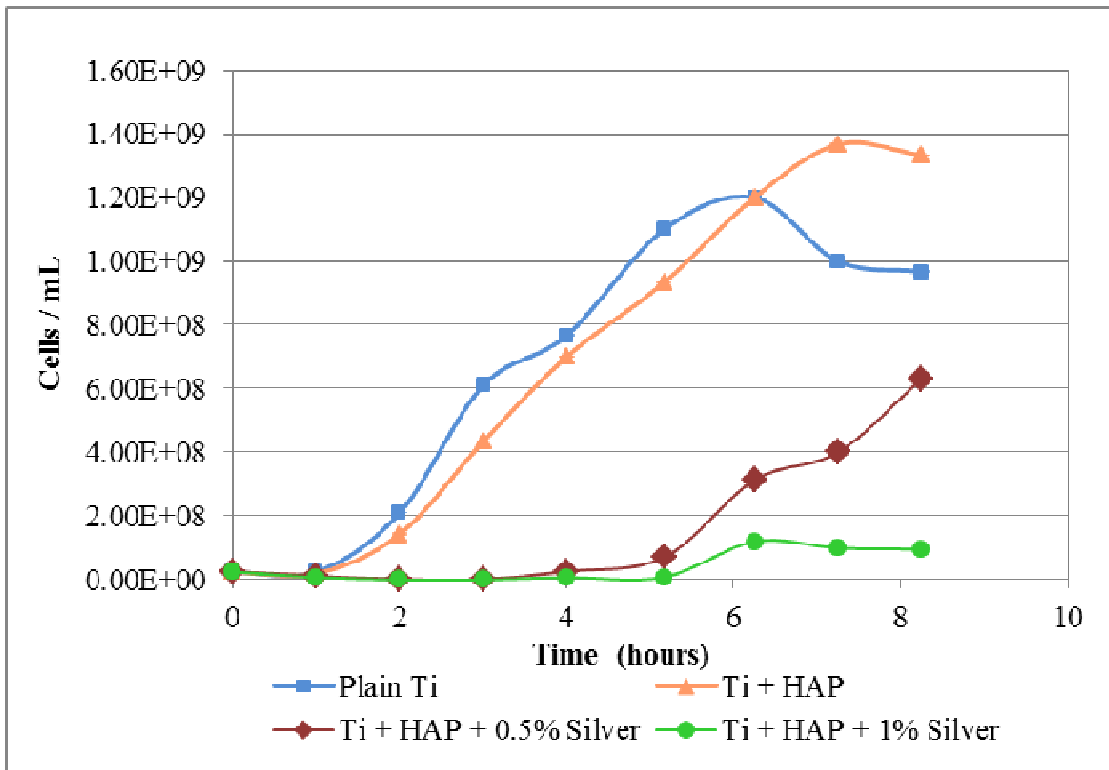


**Figure 26:** Growth of *SE* bacteria cells over 8 hours in solution

Figure 27, shows the growth of *PA* cells over 8 hours in suspension with the four substrate groups. As seen from the figure, the *PA* cells displayed a more favorable

reaction to the silver in the solution. The control groups showed a steady climb in *PA* cell growth until about 5 hours when the rate of cell growth began to increase further. The *PA* cells reaction to the delaminated substrates containing silver displayed nearly no increases in bacteria growth over the 8 hour study. Near 7 hours, the *PA* cells with the low wt% silver substrates had minimal growth while the *PA* cells with the high wt% silver substrates remained at a flat-line for the entire 8 hours. It appears from these results that silver may have a higher effect on gram negative aerobic bacteria than gram positive aerobic bacteria.

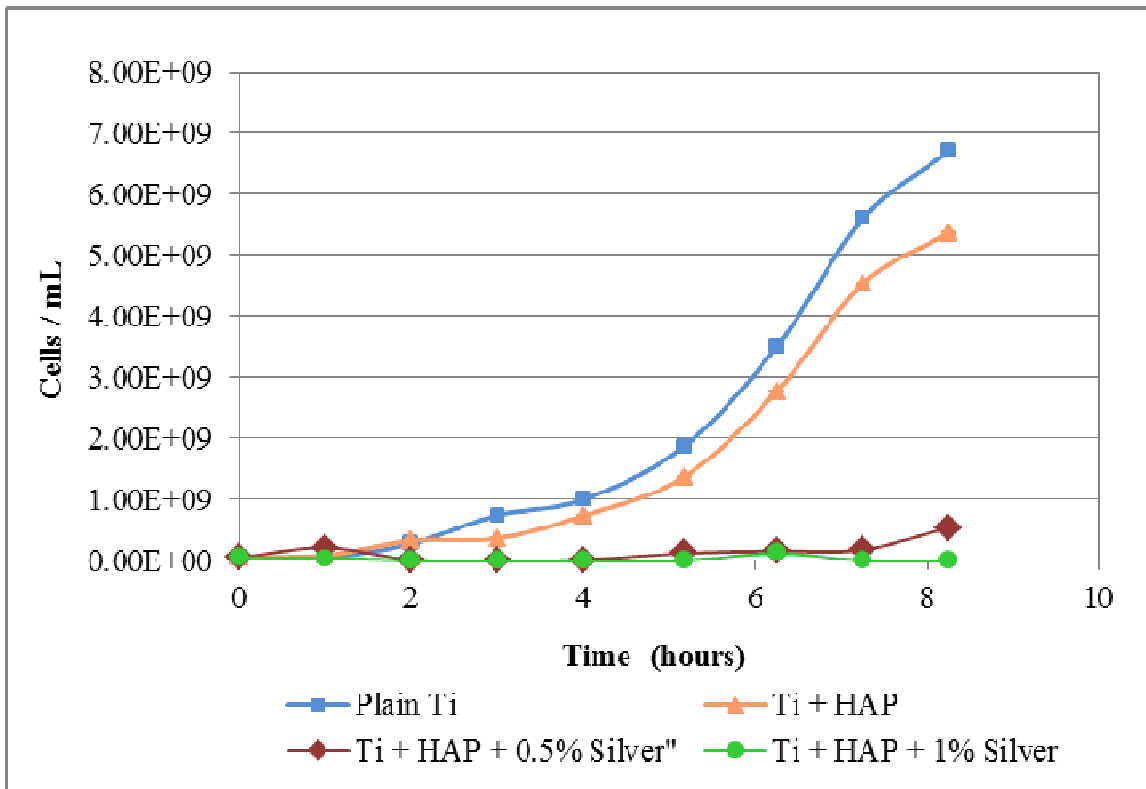


**Figure 27:** Growth of *PA* bacteria cells over 8 hours in solution

## CHAPTER 5: PRELIMINARY ANNEALING AND HIGH TEMPERATURE TREATMENTS OF THE THIN FILMS

This chapter outlines the methods, materials, results and discussion of annealing and high temperature treatments of substrates sputter coated with silver-doped thin films. These preliminary studies were conducted in order to determine if the stability of the films could be improved while maintaining the silver concentrations within the films. Once again the samples were subjected to physical and mechanical characterization tests as previously used which included scanning electron microscopy, energy dispersive spectroscopy, adhesion testing using ASTM D3359-09, and stability testing using incubated PBS immersion.

### 5.1: METHODS AND MATERIALS

Increasing stability and resistance of the films to overcome strong destabilizing forces while in aqueous environments was essential after the as-sputtered films performed poorly in those conditions. This study examined the use of various heat treatments on the sputter deposited thin films in order to increase the crystallinity of the hydroxyapatite. The first attempted method involved subjecting the titanium substrates to heat treatment during sputter deposition of the hydroxyapatite/silver target in order to be crystallizing the hydroxyapatite after making contact with the etched titanium. The sample holder shown in Figure 28 was fabricated out of a 2 in. wide 4 in. long stainless steel block with a thickness of 0.5 in. Three 0.5 in wide channels were milled across the

back of the sample holder in order to install three heater cartridges. The heater cartridges were made out of three 6 in. long alumina ceramic tubes, coiled nickel chromium resistance wire and thermal conductive hi-resistance potting compound. The nickel chromium wire was stretched to a length of 6 in. with a resistance of 3 ohms per cartridge. The resistance wire was fed into the alumina ceramic tubing and stabilized with potting compound. Once the potting compound was allowed to cure for 24 hours, the heater cartridges were carefully positioned within the channels of the sample holder, stabilized with the potting compound, and allowed to cure for 24 hours. Calcium-magnesium-silicate Superwool™ insulation was wrapped around the top, bottom, and back of the sample holder in order to direct the heat towards the front. The ends of all three heater cartridges were fastened with nickel plated terminal ring lugs and wired in parallel to the with the Sorenson SRL 60-35 power supply.

The desired goal temperature of the sample holder was chosen at 600°C. A type K thermocouple was temporarily spot-welded to the sample holder to determine the amount of power needed to drive the samples up to a temperature of 600°C. Once the necessary power was determined to keep the sample holder at steady state in vacuum, the thermocouple was removed to sputter deposit silver-doped hydroxyapatite thin films on to etched titanium samples at 600°C.

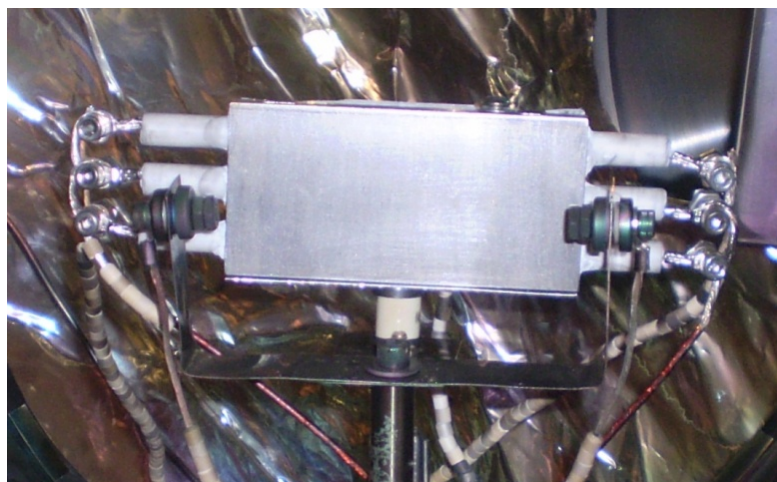


**Figure 28:** High temperature sample holder with installed heater cartridges

Titanium substrates to be sputter deposited with hydroxyapatite films doped a low weight percentage of silver at 600°C were marked with a scribe and labeled A3. Titanium substrates to be sputter deposited with hydroxyapatite films doped with a high weight percentage of silver at 600°C were marked with a scribe and labeled A4. For both groups, the maximum number of samples (n=35) were placed onto the sample holder during each 10 hour deposition. For each run, the chamber was pumped down to a pressure of  $1 \times 10^{-5}$  torr and the sample holder was slowly brought up to 600°C before turning on the ion source. The sample holder was held at 600°C for the entire duration of the sputter deposition and continued to remain at that temperature for 1 hour after deposition was completed. The sample holder and the coated titanium substrates were allowed to cool down to room temperature before venting the vacuum chamber.

The second method for increasing the crystallinity of the hydroxyapatite involved annealing in air. Similar with the previous method, substrates were marked with a scribe and labeled either A5 or A6 based on the concentration of silver to be deposited within the hydroxyapatite films. Group A5 was sputtered hydroxyapatite with low wt% of silver

and A6 was sputtered hydroxyapatite with high wt% of silver. For each run, the titanium substrates were sputter deposited at normal vacuum temperature. The coated substrates were annealed in air using a Lindberg oven (max 1200°C) at a temperature of 600°C for a period of two hours and allowing the oven and the samples to slowly cool back to room temperature.

As with the amorphous hydroxyapatite thin films, substrates were physically characterized using SEM, EDS, ASTM Standard D3359-09 Tape Testing, and incubated PBS immersion stability testing. In addition, the films were characterized using glancing angle X-ray diffraction in order to determine that a crystalline form of hydroxyapatite was present within the films.

**Table 2:** Annealed substrate group labels and descriptions

<b>Substrate Label</b>	<b>A3</b>	<b>A4</b>	<b>A5</b>	<b>A6</b>
<b>Description</b>	Etched Ti + Sputtered HAp + Low wt% Ag	Etched Ti + Sputtered HAp + High wt% Ag	Etched Ti + Sputtered HAp + Low wt% Ag	Etched Ti + Sputtered HAp + High wt% Ag
<b>Heat Treatment</b>	600°C during sputter deposition	600°C during sputter deposition	600°C in air for 2 hours	600°C in air for 2 hours

## 5.2: RESULTS AND DISCUSSION

The results from EDS on the coated samples subjected to high temperature processing during deposition determined that there was little to no silver present within the films. The average quantitative values from the EDS spectrum displayed concentrations of silver lower than 0.10 wt% on substrates from both A3 and A4. In

addition to the silver, lower amounts of calcium and phosphorus were sputter deposited onto the titanium substrates which resulted in a thinner film than 600nm. Although the vapor pressure of silver at 600°C is near  $10^{-7}$  torr and the pressure of the chamber during sputter deposition was near  $10^{-4}$  torr, it is assumed that the silver was diffusing out of the film almost as fast as it was being deposited which is why concentration of silver was so low for both groups. SEM images of the substrates revealed that the temperature treatment during deposition created completely different micro scale and nano-scale topographies from the amorphous films (Figure 29). Due to the results from EDS and SEM, it was concluded that this heat treatment procedure needed to be discarded or modified in order to be effective for increasing hydroxyapatite crystallinity with silver-doped thin films. Further tests were not carried out with groups A3 and A4.

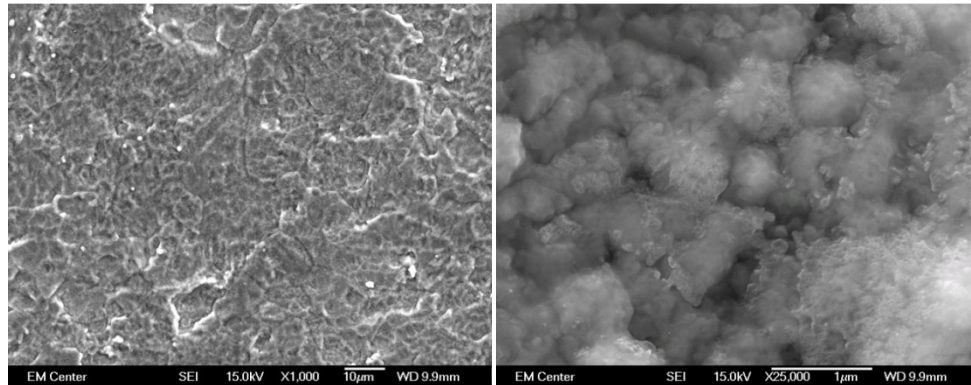


**Figure 29:** Substrates subjected to high temperature during sputter deposition

Quantitative results from EDS of the substrates subjected to annealing in air after sputter deposition showed that the silver concentrations in the films remained unchanged after heat treatment (Figure 30). The sputtered silver particles remained intact in the film during crystallization of the hydroxyapatite at 600°C. Figure 31 shows the spectral imaging and distribution of silver for both groups before and after annealing. As shown

in the figure, there is no significant difference between the amorphous films and the crystalline films regarding silver concentrations and distribution. SEM images of the A5 and A6 (Figure32) showed that small cracks had formed in the films after annealing. It is possible that these cracks formed due to residual stresses in the films during heat treatments or differences in thermal expansion between the titanium and the hydroxyapatite.

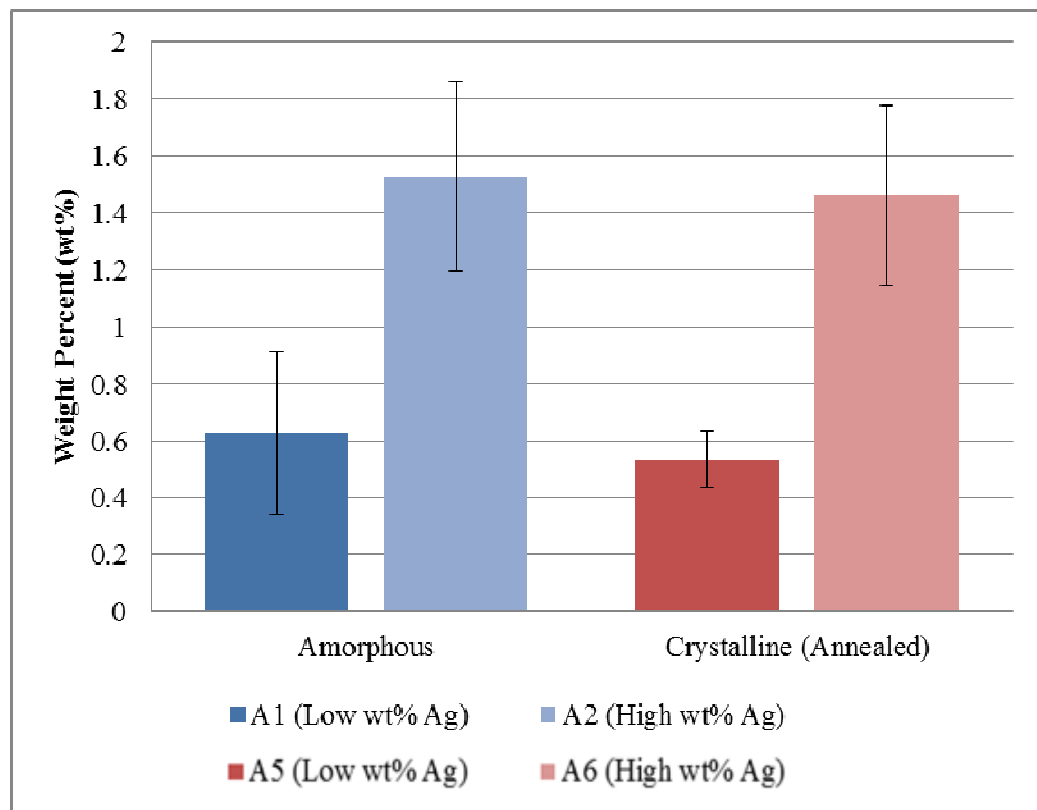


**Figure 30:** Comparison of amorphous and crystalline silver-doped HAp thin films

**A3:**Hydroxyapatite + Low wt% Ag

**A4:** Hydroxyapatite + High wt% Ag

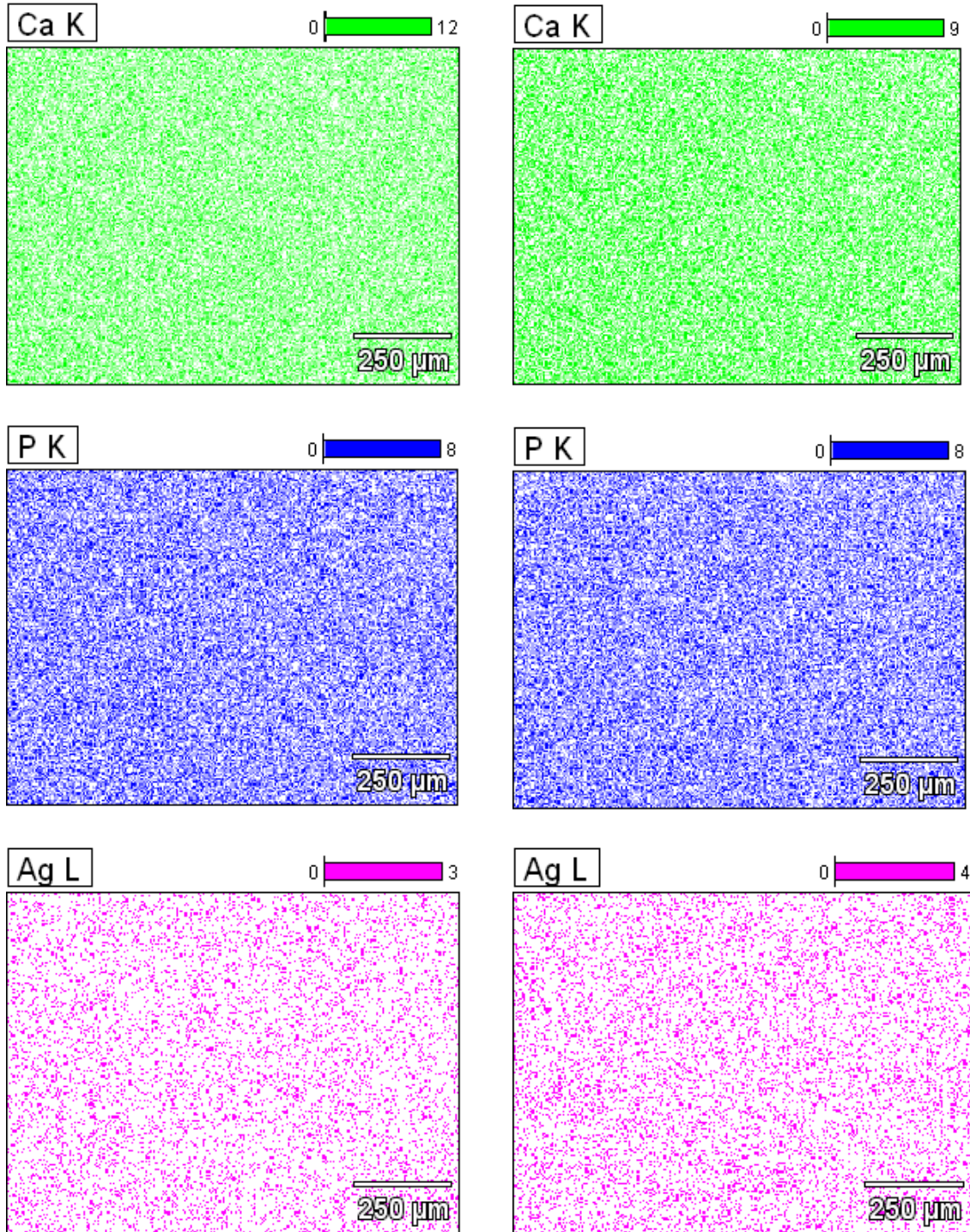


**Figure 31:** Spectral imaging of substrate groups A3 and A4

**A3:** Hydroxyapatite + Low wt% Ag

**A4:** Hydroxyapatite + High wt% Ag

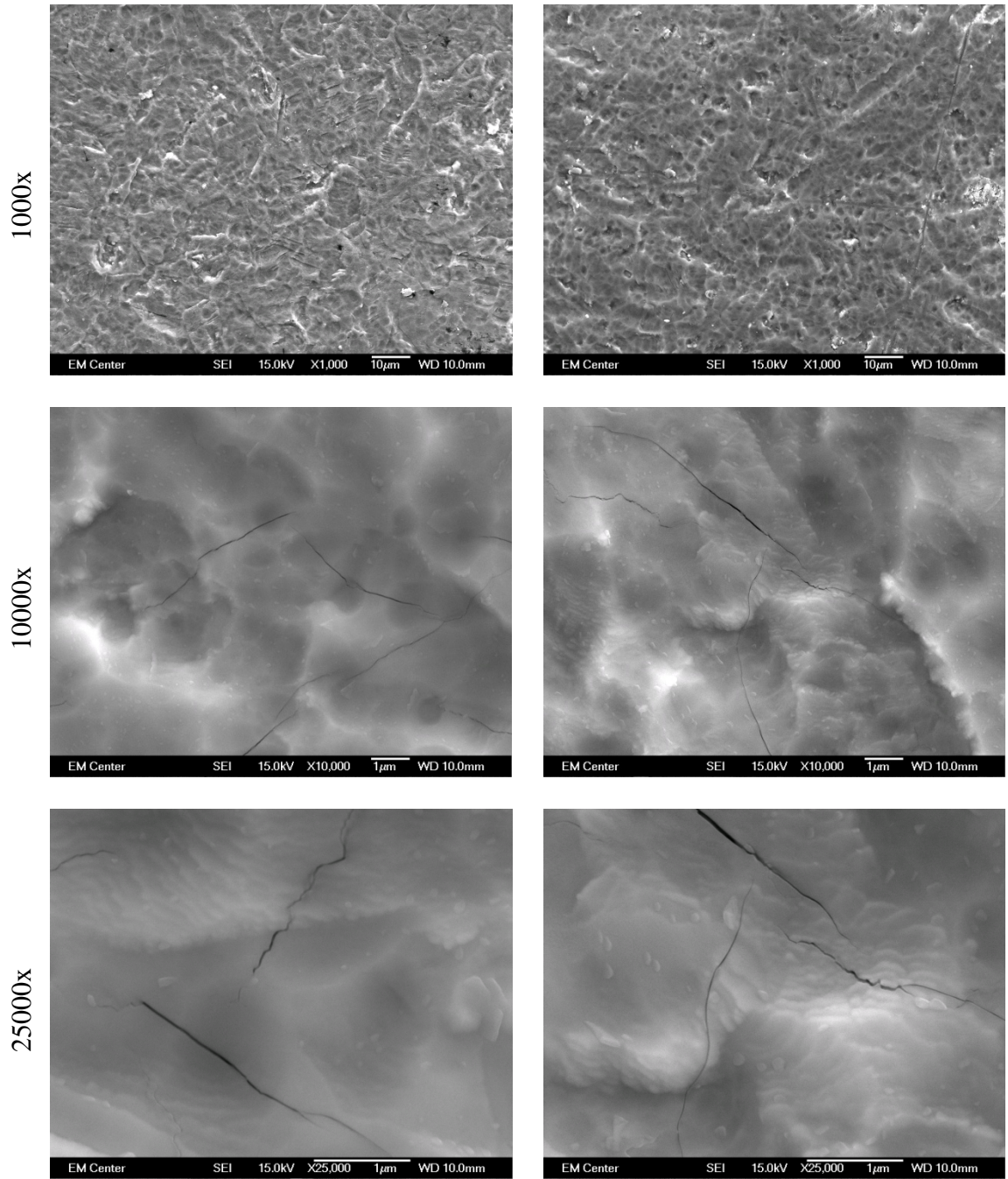


**Figure 32:** SEM images of annealed silver-doped hydroxyapatite films on etched Ti

Figures 33 and 34 are the glancing angle X-ray diffraction scans for the two substrate groups annealed in air. Figure 30 is the etched titanium sputtered with the low wt% silver-doped hydroxyapatite film and Figure 31 is the etched titanium sputtered with the high wt% silver-doped hydroxyapatite film. In both scans, the film displays peaks corresponding to the titanium substrate (purple), hydroxyapatite (red), and silver (green). Although the hydroxyapatite peaks are significant, it is unclear to tell whether the hydroxyapatite is 100% crystalline. However the presence of these peaks assures that the films have undergone a significant amount of recrystallization.

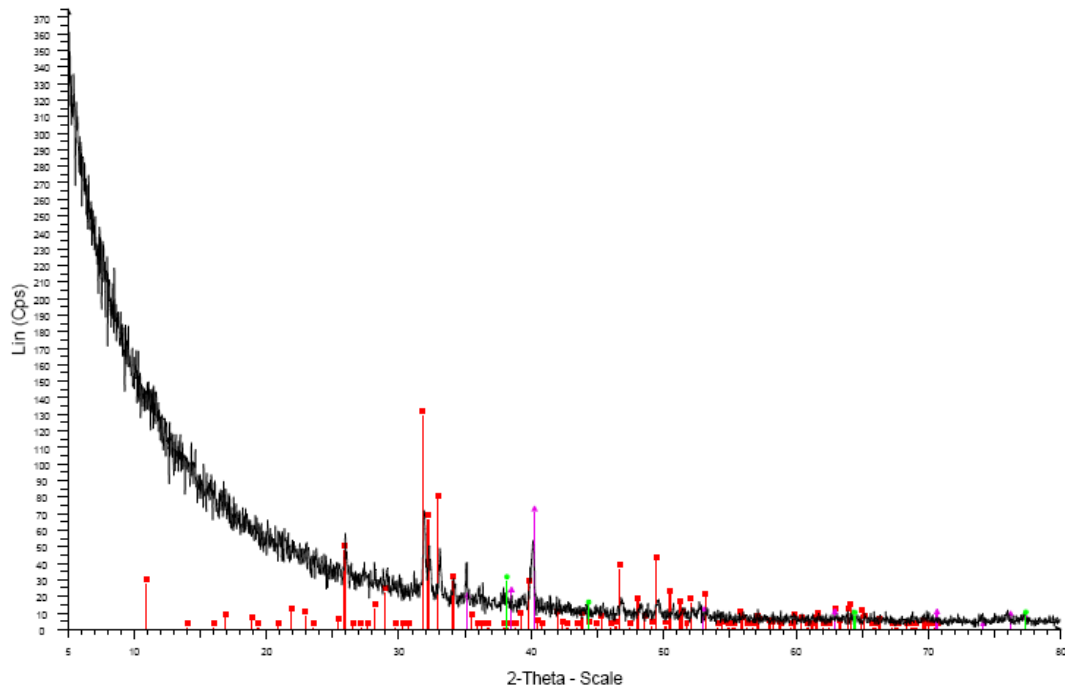
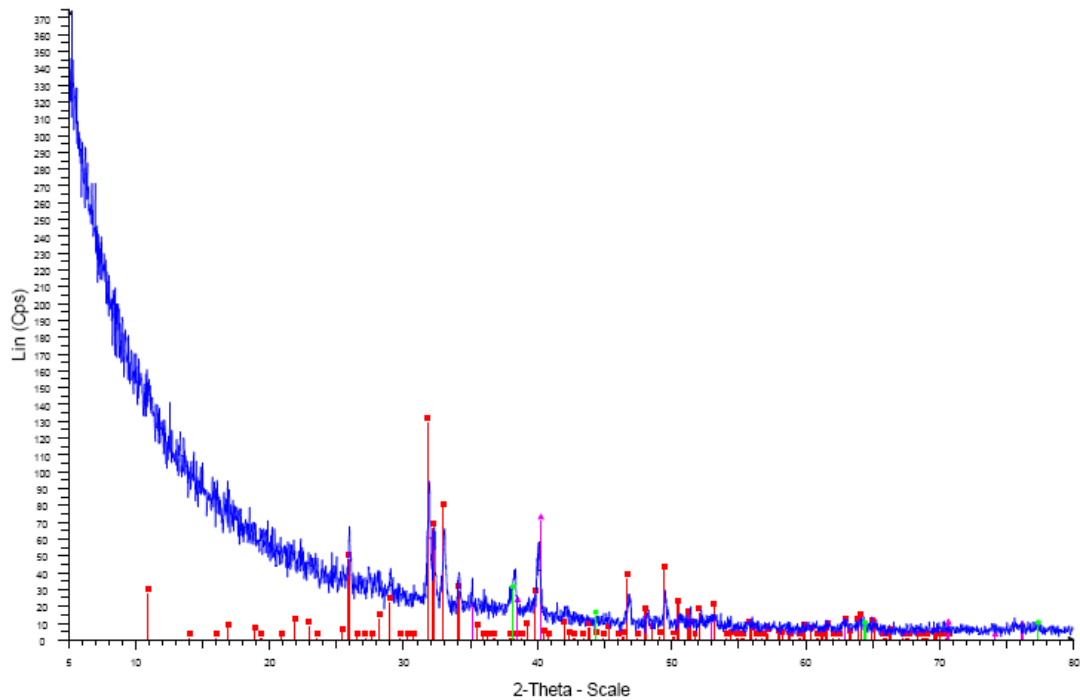


**Figure 33:** XRD scan of annealed 0.5 wt% silver-doped hydroxyapatite film substrate



after the 4 week stability study that silver concentrations for A5 and A6 were  $0.65 \text{ wt}\% \pm 0.23$  and  $1.47 \text{ wt}\% \pm 0.49$  respectively. This indicated that no silver leaching of the annealed films was occurring while in aqueous conditions for long-term periods.

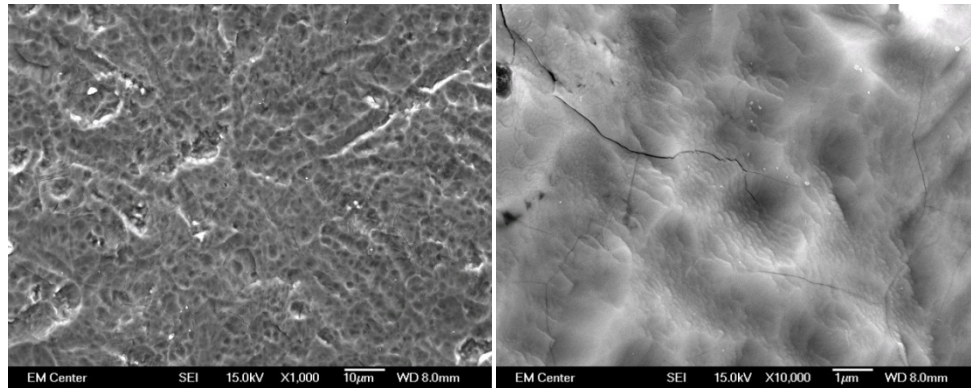


**Figure 35:** No delamination or damage of the annealed film from PBS immersion

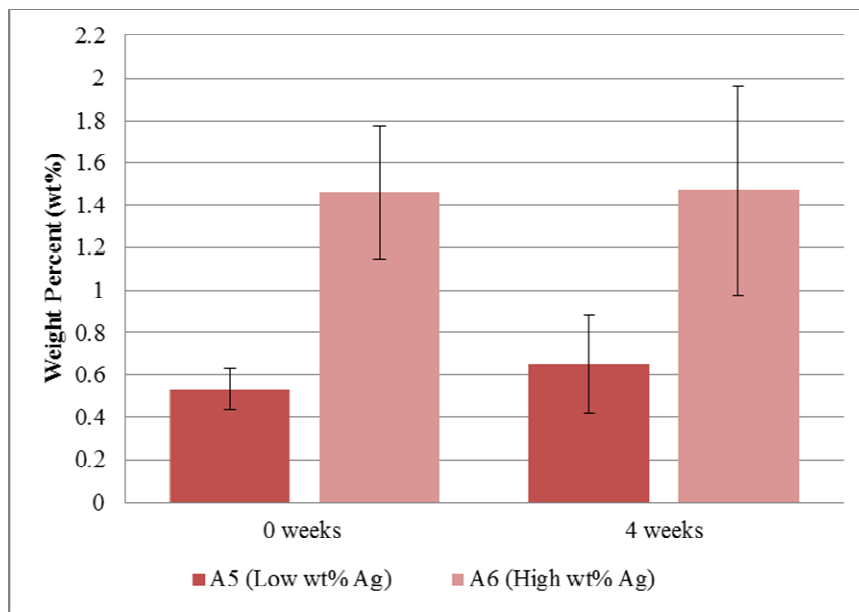


**Figure 36:** Comparison of silver wt% before and after 4 week stability studies in PBS

## CHAPTER 6: CONCLUSIONS AND FUTURE WORK

Overall, this study has provided excellent insight into the importance of plasma engineering techniques to positively modify the surface of biomaterials for prevention of biofilm formation as well as create potential for enhanced osseointegration. Pulse biased plasma etching procedures on titanium substrates provided the ability to create a textured surface with features on the micro-scale and nano-scale that are similar to ion beam etching which has been shown to create topographies advantageous for cell proliferation and differentiation into bone cells. In addition, pulse biased plasma etching also significantly decreased the amount of processing due to higher plasma densities which allowed for more ion bombardment.

Through this study, plasma engineering of biomaterials has also shown the advantages of using ion beam sputtering techniques to successfully coat the surfaces of titanium with thin films of hydroxyapatite doped with antimicrobial silver particles. Physical characterization of these thin films showed that it is possible to control the concentration of silver that is doped within the hydroxyapatite film as well as manage the uniformity and even distribution of silver across the entire surface of the film. Though the films were not shown to be 100% stable in their amorphous form, they still provided significant effects in suspension against the growth of Gram-positive *Staphylococcus epidermidis* and Gram-negative *Pseudomonas aeruginosa* which are well known pathogens that often create infections with orthopedic devices and implants. Heat treatments such as annealing in air were revealed to increase the stability of the films in

both dry and aqueous environments without disturbing or losing the concentration of silver within the sputtered hydroxyapatite films.

Future work to be done in this area includes many short term and long term projects that would help further this research to eventually developing a thin film coating on medical devices and implants used in the operating room. First, further investigations on the understanding the physical characterization of the films may be done by looking at the film response to other mechanical and chemical forces that were not tested in this study. These tests may include scratch testing, nanoindentation, and stability of the films cell culture media. In addition, a future short term project would be to investigate the behavior of bacteria on the heat treated films to see if there is a similar response to the silver using not only *SE* and *PA* cells, but also other Gram-positive and Gram negative pathogens which affect oral, craniofacial, and dental implants as well. Although it is suggested that the silver should have no negative effect on the proliferation and differentiation of mesenchymal stem cells on the surface of the substrates, 4-week cell studies would be included as another future project related to the biological characterization of the films. Finally, long term goals would be to use plasma immersion, pulse bias, and ion beam sputtering to pre-etch and uniformly sputter coat three dimensional objects with thin films of hydroxyapatite doped with silver particles and optimize the procedure to be fast yet producing the same quality of films.

## WORKS CITED

1. Chen, W., et al., *In vitro anti-bacterial and biological properties of magnetron co-sputtered silver-containing hydroxyapatite coating*. *Biomaterials*, 2006. 27(32): p. 5512-5517.
2. Kim, S., *Changes in surgical loads and economic burden of hip and knee replacements in the US: 1997-2004*. *Arthritis & Rheumatism-Arthritis Care & Research*, 2008. 59(4): p. 481-488.
3. Fehring, T.K., et al., *Early failures in total knee arthroplasty*. *Clinical Orthopaedics and Related Research*, 2001(392): p. 315-318.
4. Dobzyniak, M., T.K. Fehring, and S. Odum, *Early failure in total hip arthroplasty*. *Clinical Orthopaedics and Related Research*, 2006(447): p. 76-78.
5. Losina, E., et al., *Early failures of total hip replacement - Effects of surgeon volume*. *Arthritis and Rheumatism*, 2004. 50(4): p. 1338-1343.
6. Chua, P.H., et al., *Surface functionalization of titanium with hyaluronic acid/chitosan polyelectrolyte multilayers and RGD for promoting osteoblast functions and inhibiting bacterial adhesion*. *Biomaterials*, 2008. 29(10): p. 1412-1421.
7. Popat, K.C., et al., *Decreased Staphylococcus epidermis adhesion and increased osteoblast functionality on antibiotic-loaded titania nanotubes*. *Biomaterials*, 2007. 28(32): p. 4880-4888.
8. Moioli, E.K., et al., *Matrices and scaffolds for drug delivery in dental, oral and craniofacial tissue engineering*. *Advanced Drug Delivery Reviews*, 2007. 59(4-5): p. 308-324.
9. Chua, P.H., et al., *Structural stability and bioapplicability assessment of hyaluronic acid-chitosan polyelectrolyte multilayers on titanium substrates*. *Journal of Biomedical Materials Research Part A*, 2008. 87A(4): p. 1061-1074.
10. Ng, A.M.H., et al., *Differential osteogenic activity of osteoprogenitor cells on HA and TCP/HA scaffold of tissue engineered bone*. *Journal of Biomedical Materials Research Part A*, 2008. 85A(2): p. 301-31

11. Ong, J.L., et al., *The characterization and development of bioactive hydroxyapatite coatings*. Jom, 2006. 58(7): p. 67-69.
12. Huang, J., et al., *In vitro assessment of the biological response to nano-sized hydroxyapatite*. Journal of Materials Science-Materials in Medicine, 2004. 15(4): p. 441-445.
13. Rabiei, A., et al., *Microstructure, mechanical properties, and biological response to functionally graded HA coatings*. Materials Science & Engineering C- Biomimetic and Supramolecular Systems, 2007. 27(3): p. 529-533.
14. Furlong, R.J. and J.F. Osborn, *FIXATION OF HIP PROSTHESES BY HYDROXYAPATITE CERAMIC COATINGS*. Journal of Bone and Joint Surgery-British Volume, 1991. 73(5): p. 741-745.
15. Yang, Y.Z., K.H. Kim, and J.L. Ong, *Review on calcium phosphate coatings produced using a sputtering process - an alternative to plasma spraying*. Biomaterials, 2005. 26(3): p. 327-337.
16. Hong, Z.D., et al., *Crystalline hydroxyapatite thin films produced at room temperature - An opposing radio frequency magnetron sputtering approach*. Thin Solid Films, 2007. 515(17): p. 6773-6780.
17. Sanden, B., et al., *Hydroxyapatite coating improves fixation of pedicle screws - A clinical study*. Journal of Bone and Joint Surgery-British Volume, 2002. 84B(3): p. 387-391.
18. Epinette, J.A. and M.T. Manley, *Fifteen years of clinical experience with hydroxyapatite coatings in joint arthroplasty*. 2004, Paris: Springer. xvi, 452 p.
19. Nelissen, R.G.H.H., E.R. Valstar, and P.M. Rozing, *The effect of hydroxyapatite on the micromotion of total knee prostheses - A prospective, randomized, double-blind study*. Journal of Bone and Joint Surgery-American Volume, 1998. 80A(11): p. 1665-1672.
20. Capello, W.N., et al., *Hydroxyapatite-coated total hip femoral components in patients less than fifty years old - Clinical and radiographic results after five to eight years of follow-up*. Journal of Bone and Joint Surgery-American Volume, 1997. 79A(7): p. 1023-1029.
21. Sun, L.M., et al., *Material fundamentals and clinical performance of plasma-sprayed hydroxyapatite coatings: A review*. Journal of Biomedical Materials Research, 2001. 58(5): p. 570-592.

22. Lee, J.H., et al., *Microfluidic Approach to Create Three-Dimensional Tissue Models for Biofilm-Related Infection of Orthopaedic Implants*. Tissue Engineering Part C-Methods, 2011. 17(1): p. 39-48.
23. Campoccia, D., L. Montanaro, and C.R. Arciola, *The significance of infection related to orthopedic devices and issues of antibiotic resistance*. Biomaterials, 2006. 27(11): p. 2331-2339.
24. Simionescu, R.E. and D.J. Kennedy, *Prevention of Infection in Prosthetic Devices*, in *The Bionic Human*, F.E. Johnson, et al., Editors. 2006, Humana Press. p. 159-185.
25. Bernard, L., et al., *Trends in the treatment of orthopaedic prosthetic infections*. Journal of Antimicrobial Chemotherapy, 2004. 53(2): p. 127-129.
26. Gillespie, W.J. and G.H. Walenkamp, *Antibiotic prophylaxis for surgery for proximal femoral and other closed long bone fractures*. Cochrane Database Syst Rev, 2010(3): p. CD000244.
27. Chu, V.H., et al., *Staphylococcus aureus bacteremia in patients with prosthetic devices: costs and outcomes*. Am J Med, 2005. 118(12): p. 1416.
28. Lansdown, A.B., *Critical observations on the neurotoxicity of silver*. Crit Rev Toxicol, 2007. 37(3): p. 237-50.
29. Atiyeh, B.S., et al., *Effect of silver on burn wound infection control and healing: review of the literature*. Burns, 2007. 33(2): p. 139-48.
30. Silver, S., *Bacterial silver resistance: molecular biology and uses and misuses of silver compounds*. FEMS Microbiol Rev, 2003. 27(2-3): p. 341-53.
31. Lansdown, A.B., *Silver in health care: antimicrobial effects and safety in use*. Curr Probl Dermatol, 2006. 33: p. 17-34.
32. Darouiche, R.O., *Anti-infective efficacy of silver-coated medical prostheses*. Clinical Infectious Diseases, 1999. 29(6): p. 1371-1377.
33. Ewald, A., et al., *Antimicrobial titanium/silver PVD coatings on titanium*. Biomedical Engineering Online, 2006. 5: p. -.
34. Zheng, X., et al., *Antibacterial Property and Biocompatibility of Plasma Sprayed Hydroxyapatite/Silver Composite Coatings*. Journal of Thermal Spray Technology, 2009: p. 1-6.

35. Chen, W., et al., *Antibacterial and osteogenic properties hydroxyapatite coatings produced using of silver-containing a sol gel process*. Journal of Biomedical Materials Research Part A, 2007. 82A(4): p. 899-906.
36. Cooley, D.R., et al., *The Advantages of Coated Titanium Implants Prepared by Radiofrequency Sputtering from Hydroxyapatite*. Journal of Prosthetic Dentistry, 1992. 67(1): p. 93-100.
37. Lucas, L.C., et al., *Calcium-Phosphate Coatings for Medical and Dental Implants*. Colloids and Surfaces a-Physicochemical and Engineering Aspects, 1993. 77(2): p. 141-147.
38. Wolke, J.G.C., et al., *Study of the Surface Characteristics of Magnetron-Sputter Calcium-Phosphate Coatings*. Journal of Biomedical Materials Research, 1994. 28(12): p. 1477-1484.
39. Shi, J.Z., et al., *Application of magnetron sputtering for producing bioactive ceramic coatings on implant materials*. Bulletin of Materials Science, 2008. 31(6): p. 877-884.
40. Riedel, Nicholas A. *Sputter Deposited Hydroxyapatite Thin Films For Enhanced Osseointegration*. MS Thesis. Colorado State University, Fort Collins, CO, 2010. Print.